Cell Reports

Article

Spatio-molecular profiles shape the human cerebellar hierarchy along the sensorimotor-association axis

Graphical abstract

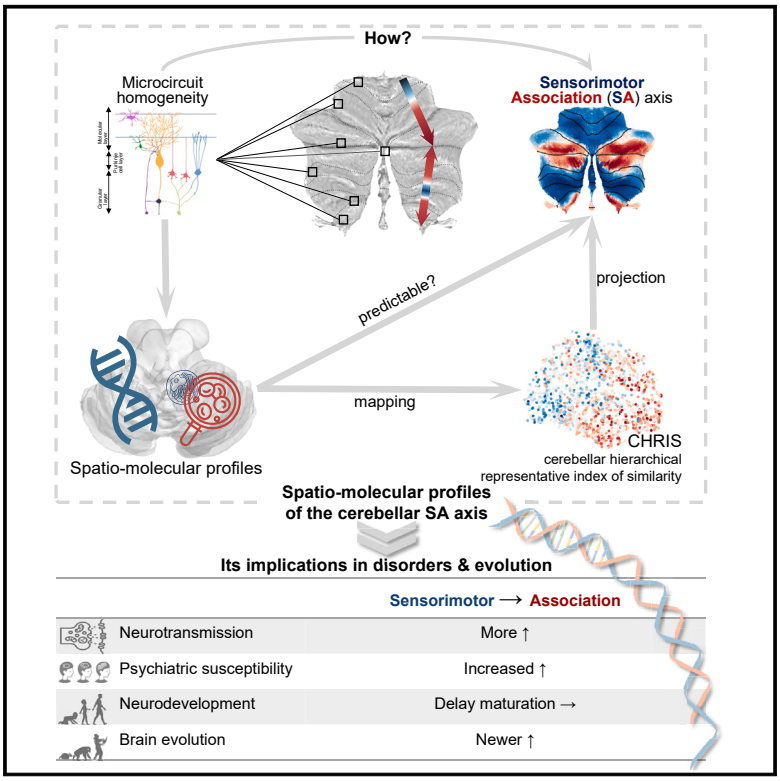

Highlights

- The functional hierarchy of the cerebellum is represented in its spatio-molecular profiles
- Identified genes engage in psychiatric disorders, neurodevelopment, and brain evolution
- The spatio-molecular profiles establish the cerebello-cerebral correspondence in SA axis

Authors

Yaping Wang, Yufan Wang, Haiyan Wang, ..., Kristoffer Hougaard Madsen, Congying Chu, Lingzhong Fan

Correspondence

chucongying@gmail.com (C.C.), lingzhong.fan@ia.ac.cn (L.F.)

In brief

Wang et al. investigate the genetic underpinnings of the functional hierarchy along the sensorimotor-association axis in the human cerebellum. These gene-to-hierarchy associations are connected to neurotransmission, neuropsychiatric disorders, brain development, and brain evolution, aligning with the cerebral cortical hierarchy.

Wang et al., 2024, Cell Reports *43*, 113770
February 27, 2024
https://doi.org/10.1016/j.celrep.2024.113770

CellPress

Cell Reports

CellPress
OPEN ACCESS

Article

Spatio-molecular profiles shape the human cerebellar hierarchy along the sensorimotor-association axis

Yaping Wang,[1,2] Yufan Wang,[2] Haiyan Wang,[2] Liang Ma,[2] Simon B. Eickhoff,[5,6] Kristoffer Hougaard Madsen,[1,7,8] Congying Chu,[2,*] and Lingzhong Fan[1,2,3,4,9,*]

[1]Sino-Danish Center, University of Chinese Academy of Sciences, Beijing 100190, China
[2]Brainnetome Center, Institute of Automation, Chinese Academy of Sciences, Beijing 100190, China
[3]CAS Center for Excellence in Brain Science and Intelligence Technology, Institute of Automation, Chinese Academy of Sciences, Beijing 100190, China
[4]School of Health and Life Sciences, University of Health and Rehabilitation Sciences, Qingdao 266000, China
[5]Institute of Neuroscience and Medicine (INM-7: Brain and Behaviour), Research Centre Jülich, 52425 Jülich, Germany
[6]Institute of Systems Neuroscience, Heinrich Heine University Düsseldorf, 40225 Düsseldorf, Germany
[7]Department of Applied Mathematics and Computer Science, Technical University of Denmark, 2800 Kongens Lyngby, Denmark
[8]Danish Research Centre for Magnetic Resonance, Centre for Functional and Diagnostic Imaging and Research, Copenhagen University Hospital-Amager and Hvidovre, 2650 Hvidovre, Denmark
[9]Lead contact
*Correspondence: chucongying@gmail.com (C.C.), lingzhong.fan@ia.ac.cn (L.F.)
https://doi.org/10.1016/j.celrep.2024.113770

SUMMARY

Cerebellar involvement in both motor and non-motor functions manifests in specific regions of the human cerebellum, revealing the functional heterogeneity within it. One compelling theory places the heterogeneity within the cerebellar functional hierarchy along the sensorimotor-association (SA) axis. Despite extensive neuroimaging studies, evidence for the cerebellar SA axis from different modalities and scales was lacking. Thus, we establish a significant link between the cerebellar SA axis and spatio-molecular profiles. Utilizing the gene set variation analysis, we find the intermediate biological principles the significant genes leveraged to scaffold the cerebellar SA axis. Interestingly, we find these spatio-molecular profiles notably associated with neuropsychiatric dysfunction and recent evolution. Furthermore, cerebello-cerebral interactions at genetic and functional connectivity levels mirror the cerebral cortex and cerebellum's SA axis. These findings can provide a deeper understanding of how the human cerebellar SA axis is shaped and its role in transitioning from sensorimotor to association functions.

INTRODUCTION

Beyond its traditional role in motor coordination, the human cerebellum is extensively involved in higher-order non-motor functions, such as cognition and emotion.[1,2] Coming to understand this inspired a compelling theory that situates the functional diversity within the cerebellar functional hierarchy along the sensorimotor-association (SA) axis,[3] a concept well established in the cerebral cortex.[4] The SA axis is well portrayed by the functional gradient (FG)[5] using functional neuroimaging, which follows a progression from motor to attentional/executive to involvement in the default-mode network. The presence of the cerebellar SA axis provides valuable insights into the functional role of the human cerebellum and its contribution to overall brain function.[5–7] It sheds light on how the cerebellum influences ongoing actions and prepares for future goals[8] while also serving as a research paradigm for understanding clinical functional impairments.[9] However, despite studies confirming the existence and clinical significance of the cerebellar SA axis using functional imaging, there remains a lack of evidence from different modalities and scales to support the existence of the axis and reveal its biological relevance.

The human cerebellum has long been found to have a relatively uniform intrinsic microcircuitry.[1] How can a highly similar cellular constructure co-occur with the human cerebellar SA axis? On the one hand, the functional differentiation of the human cerebellum has been thought to be primarily derived from extracerebellar connections.[1,10] This can be initially appreciated by the massive anatomical connections between the cerebellum and the cerebral cortex and subcortical structures.[11–14] The anterior lobe of the cerebellum, which corresponds to the somatomotor function, possesses polysynaptic projections to the cerebral motor region,[15–17] while cerebellar regions related to associative functions, such as Crus I and Crus II, establish connections with the cerebral association cortex.[15,18] On the other hand, accumulating evidence in animals reveals microstructural differences between the motor and non-motor regions of the cerebellum via a variety of techniques, including

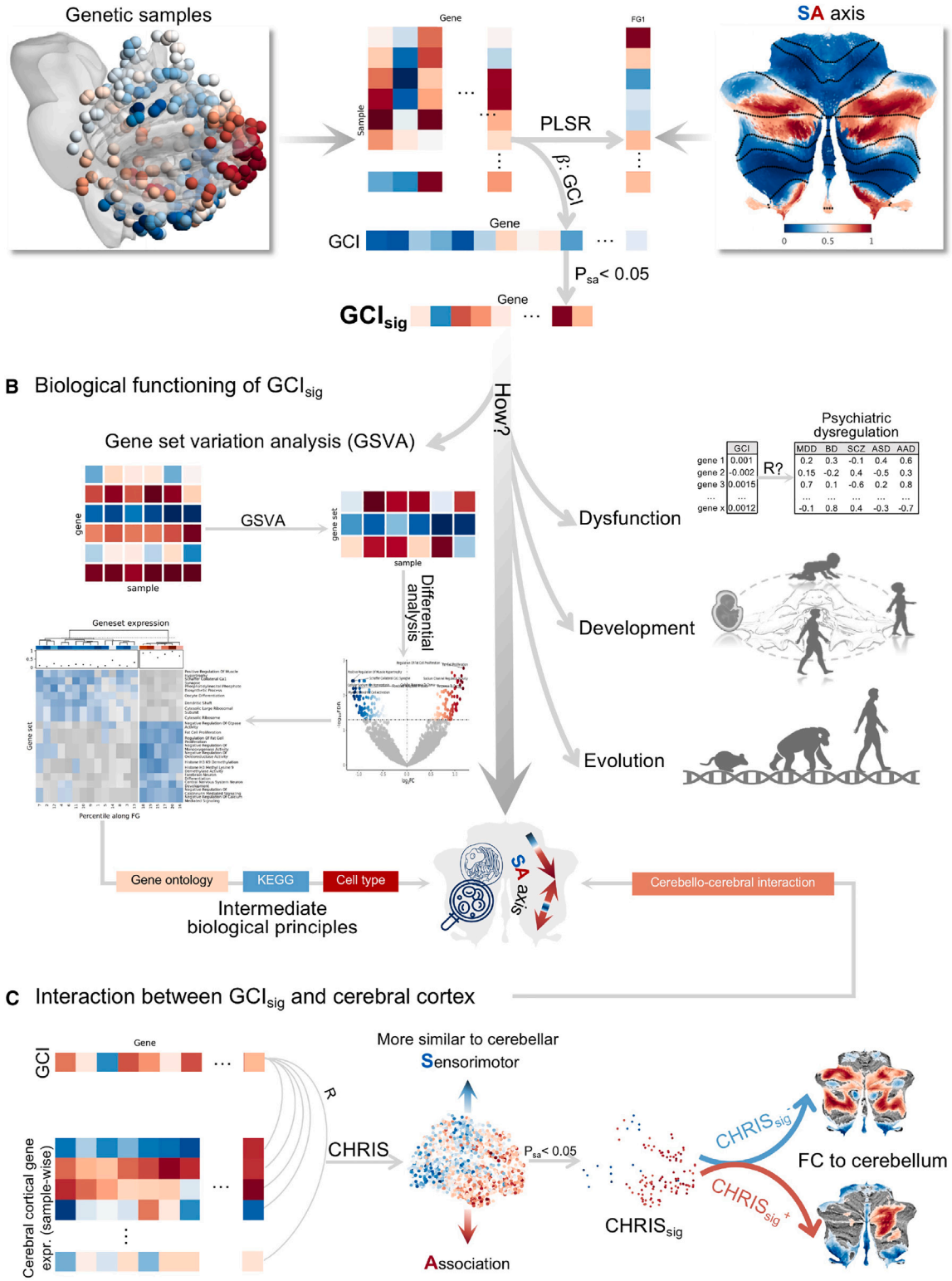

(legend on next page)

differences in zebrin patterns,[19] firing frequencies,[20] and cell-type specialization[21] among others. This suggests that microscale variations may serve as evidence in favor of another modality and scale for the human cerebellar SA axis.[2] Although the intrinsic microcircuitry of the human cerebellum has long been believed to be highly homogeneous,[1] it is possible that subtle microscale variations, similar to those observed in animal models, exist within the context of high microcircuit homogeneity.[2,22] As yet, such explorations have been severely precluded from humans because most of these techniques can only be implemented in animals, and the direct extrapolation of findings to the human cerebellum is hindered by species-specific features.[23,24]

Imaging-transcriptomics analysis has emerged as a promising approach for bridging these knowledge gaps[25–27] by integrating microscopic transcriptome data with macroscopic neuroimaging phenotypes to enable brain-wide spatial analysis.[28,29] It enhances our understanding of the molecular patterns underlying the human cerebellar functional organization,[30] offering insights beyond those from animal studies. However, current imaging-transcriptomics studies often rely on spatially correlated genes and bioinformatics databases to explain their functions, ignoring the detailed relationship between the biological function of genes and imaging phenotypes.[29] To address this limitation, gene set variation analysis (GSVA) offers a more comprehensive approach.[31] GSVA detects subtle biological activity changes by transforming gene expression data into a gene set × sample matrix,[31] enabling a functional gene-unit-centric analysis that explores the underlying biological principles behind brain features. Although previous researchers have proposed the extension of GSVA for causal inference,[31] its application in spatial brain-wide studies remains limited. Incorporating GSVA with imaging transcriptomics presents a promising opportunity to identify microscale mechanisms underlying the human cerebellar SA axis and unravel the biological principles associated with the transition from sensorimotor to association functions.

This study aimed to explore the spatio-molecular profiles underlying the SA axis of the human cerebellum. The research focused on addressing three specific questions: first, do significant changes in spatial gene expression involve shaping the cerebellar SA axis (Figure 1A)? Second, what intermediate biological principles mediate the shaping of the SA axis as observed in the animal cerebella, and are there links between these molecular substrates and neurodevelopment, evolution, and neuropsychiatric disorders related to the cerebellum (Figure 1B)? Last, how do the spatio-molecular profiles interact with the cerebral cortex at both the genetic and functional connectivity (FC) levels, given that the functional diversity of the cerebellum is thought to be mainly derived from its connections with the cerebral cortex[1,3] (Figure 1C)? To elucidate this, we first used gene expression data to predict the cerebellar SA axis and to obtain a gene contribution indicator (GCI) for each gene, as well as a set of the genes with significant GCI (GCI_{sig}) by spatial auto-correlation preserved permutation. GSVA was then applied to GCI_{sig} to inquire about the intermediate biological principles and explore the link between GCI_{sig} and neuropsychiatric disorders, neurodevelopment, and evolution. Finally, we evaluated the cerebello-cerebral coordination at the genetic and FC levels based on the GCI_{sig} and found substantial coordination between the two and that they mirrored the SA axis. Taken together, the findings of this study could offer insights into the genetic, molecular, cellular, and pathways variations as well as the cerebello-cerebral interactions that underpin the human cerebellar SA axis and shed light on the significance of the SA axis and its underlying spatio-molecular profiles in neuropsychiatric disorders and evolution.

RESULTS

The SA axis characterized by the FG was significantly predicted by GCI_{sig}

The FG (Figure 2A) was defined by analyzing the similarity of all cerebellar voxels in the FC matrix between the cerebellum and extra-cerebellar structures using diffusion map embedding. The principal component resulting from this analysis (first gradient) accounted for the greatest amount of variance (0.51; Figure S1). In terms of spatial distribution, FG extended from a bilateral dissociation of lobules I–VI and VIII to the posterior part of Crus I and II and the medial part of lobule IX[7] (Figure 2A), which essentially captured the main axis of the macroscale functional organization of the cerebellum, i.e., the SA axis, ranging from motor to attention to default mode processing.[3,32] Regarding connectivity to the cerebral cortex, along the cerebellar FG, the significant positive FC to the cerebral cortical sensorimotor area was decreased, but the significant positive FC to the cerebral cortical association area was increased (Figure 2A, right). From the independent task-based fMRI studies,[32] as the need for associative functioning increased in

Figure 1. Analysis pipeline

(A) Prediction of the SA axis, which is characterized by FG, using transcriptomic gene expression to explore the genetic substrates underlying the SA axis. We assigned the voxel-wise FG (right) values to the AHBA cerebellar samples (left) to predict the sample-wise FG using transcriptome gene expression by employing PLSR. Each gene's regression coefficient was named the gene contribution indicator (GCI) to quantify the importance of each gene in the SA axis. The significance of GCI was validated using a permutation test, which conserved the spatial auto-correlation. The set of genes with significant GCI was called GCI_{sig} to represent the gene set with significant effects when predicting the cerebellar FG.

(B) The biological functioning of GCI_{sig} was used to address how the GCI_{sig} engages in shaping the SA axis. Gene set variation analysis (GSVA) was introduced to explore the underlying stepwise biological principle that scaffolds the SA axis. Multiple datasets and bioinformatic tools were leveraged to explore the link between GCI_{sig} and *ex vivo* psychiatric gene dysfunction, temporal development, and evolution rate.

(C) How does the GCI_{sig} interact with the cerebral cortex at the genetic and FC levels? We calculated the correlations between GCI_{sig} and gene expression in cerebral cortex samples (on the left). We called this value the cerebellar hierarchical representative index of similarity (CHRIS), which represents the extent to which the genomic signature of the cerebellar SA axis is reflected in the gene expression profile of a cerebral cortical sample. The significance of CHRIS was calculated using multiple comparison tests to obtain the cerebral cortex samples with significant CHRIS (the set of cerebral cortex samples with significant CHRIS was termed $CHRIS_{sig}$) to explore their FC with the cerebellum (right).

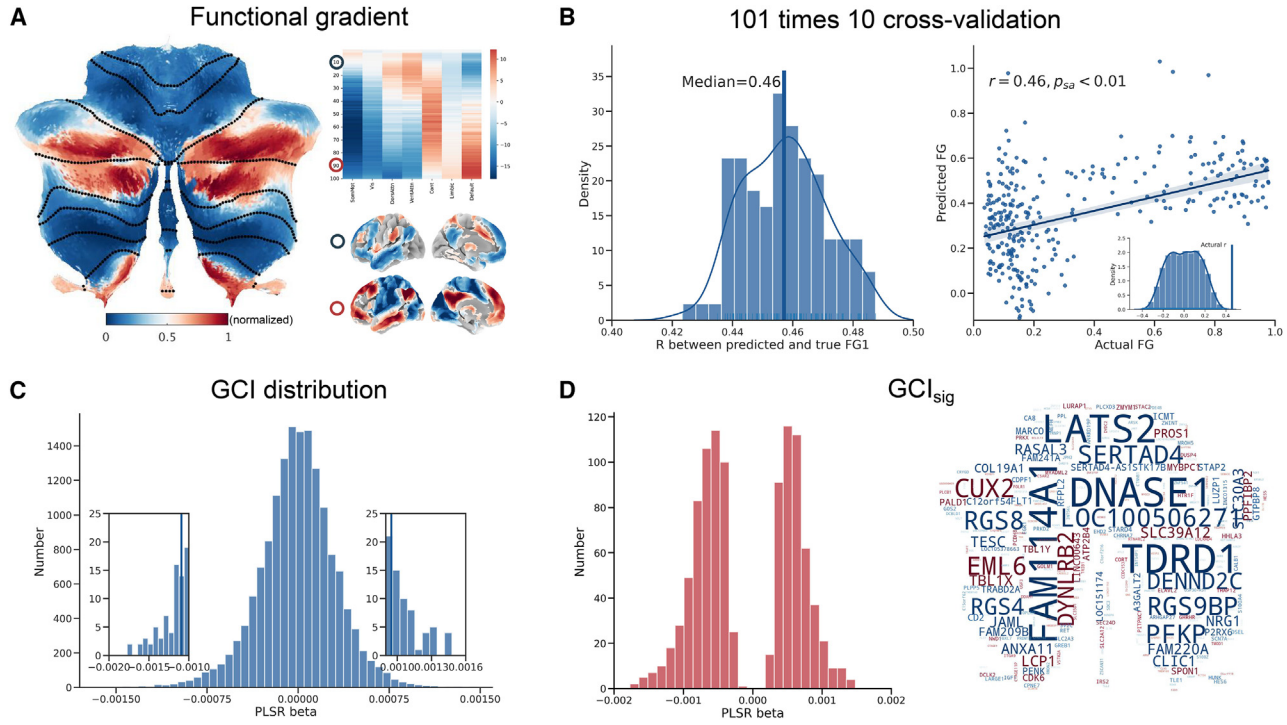

Figure 2. Prediction of the cerebellar SA axis using transcriptomic gene expression

(A) The voxel-wise FG, which captured the SA axis of the human cerebellum, was calculated using the Human Connectome Project (HCP) by decomposing the affine matrix derived from the grouped functional connectivity matrix between the cerebellum and extra-cerebellar region. The FG values were normalized to the 0–1 level. Note that we focused on the first gradient, which explained the largest amount of the variance (Figure S1). The right figure shows FC between the cerebral cortex and 100 cerebellar FG-sorted regions of interest (ROIs). The significant FC between 100 cerebellar FG-sorted ROIs with the cerebral cortex was visualized across 7 networks (top). The 7 networks were sorted by the cerebral cortical SA axis. Two of these 100 ROIs were picked to visualize the voxel-wise FC (bottom).

(B) Histogram representing the distribution of the correlation between the actual and predicted sample FG across 101× 10-fold cross-validated PLSR models (left). The median correlation (the median line in the left graph) was 0.46 (right), and the significance $p_{sa} < 0.01$ was validated using BrainSMASH (a permutation test with preserved spatial auto-correlation; embedded figure).

(C) Histogram representing the distribution of regression coefficient of each gene, which was referred to as the GCI to show the degree of importance when predicting the FG.

(D) Histogram representing the distribution of GCI_{sig} (left). The right word cloud shows the top 400 GCI_{sig} (the full list can be found in Data S1), with red representing the positive GCI_{sig} and blue representing the negative GCI_{sig}; the color density and word size represent the absolute value of GCI.

See also Figures S2 and S3.

the task (e.g., from hand pressing to distraction to word comprehension), the median FG values of the voxels within the area activated during this task also increased (Figure S1C). The correspondence between these three views, the spatial distribution pattern of the cerebellar FG and its representation across task fMRI, as well as the pattern of connectivity with the sensorimotor and associative areas of the cerebral cortex, suggests that the cerebellar FG reflects the SA axis within the cerebellum.

A partial least-squares regression (PLSR) algorithm was used to create a model predicting the FG of each sample based on its gene expression profile (Figure 1A). The optimal component number of six was chosen based on a 100×-embedded 10-fold cross-validation (CV) (Figure S2), and the prediction performance was evaluated by the median model from a 101×-embedded 10-fold CV (Figure 2B; 101× was chosen to identify the median model easily). The correlation between the predicted FG and the actual FG was 0.46 (Figure 2B) and remained significant after a permutation test, which preserved the spatial auto-correlation (we refer to the p value after this permutation test as p_{sa} [$p_{sa} < 0.01$, Figure 2B right]). In addition, a leave-one-donor-out prediction demonstrated consistency in genomic characteristics across individuals (Figure S3). All these suggest that the SA axis, as characterized by the FG, could be significantly predicted by the transcriptomic gene expression.

Next, we filtered out the significant genes that actually contributed to the FG rather than being associated by chance. The regression coefficient of each gene from the PLSR model represents the degree of contribution of each gene in predicting the FG. It thus could act as a GCI (Figure 2C). The significance of each GCI was evaluated by a permutation test, which conserved the spatial auto-correlation information from the FG, and the GCIs that survived Bonferroni correction, i.e., $p_{sa} < (0.05/15{,}624)$ were considered significant. All the genes that had a significant GCI were collectively termed the GCI_{sig} (Figure 2D).

Intermediate biological processes that the GCI_{sig} leveraged to anchor the SA axis

Since the GCI_{sig} contributes significantly to the cerebellar SA axis, how does it work? A bin-based GSVA strategy was utilized combined with the data sources included Gene Ontology (GO),[33,34] Kyoto Encyclopedia of Genes and Genomes (KEGG),[35] and cerebellar cell types data from DropViz.[36]

Combining the GO (Figure 3, blue box) and KEGG (Figure 3, orange box) results, hierarchical clustering of the samples based on the gene set enrichment score was able to clearly separate the sensorimotor from the association cerebellum. This suggests that these molecular, cellular, and pathway components vary along the SA axis and reach many levels of significant dissimilarity, especially at the two ends of the SA axis. This further revealed that distinct biological features underlie the sensorimotor and association areas of the cerebellum, as was found in experimental animal models.[19–21] Specifically, more neurotransmission processes were expressed higher in the association region, such as integral components of the presynaptic active zone membrane, calcium-mediated signaling,[37] RIG I-like receptor signaling, and hedgehog signaling pathway[38] (Figure 3; Data S3 and S4; Figures S4 and S5). Many processes that are significantly expressed in the sensorimotor cerebellum have previously been suggested to play an essential role in the motor function of the human cerebellum. These include the cytosolic ribosome, which mediates the synthesis of proteins necessary for the induction and maintenance of long-term depression in the cerebellar sensorimotor area,[39] as well as the dendritic shafts of Purkinje cells in the cerebellum, which are crucial for information processing and integration in cerebellar motor learning[40] and are in alignment with the cell-type GSVA results.

At the cell-type level, most cell types are distributed with no significant changes across the human cerebellar SA axis, which is consistent with the long-standing, largely homogeneous cytoarchitecture of the human cerebellum.[1] The only exception is the Purkinje neurons, which have a relatively higher expression in the sensorimotor area (Figure 3, green box), but this higher expression is not strong enough to dissociate the sensorimotor from the association cerebellum (Figure S6). Most of the sensorimotor cerebellum has a relatively high presence of Purkinje neurons, which is consistent with the close relationship between these neurons and motor behavior, which has been widely investigated.[1,41] In contrast, the expression of Purkinje neurons in the association cerebellum was relatively lower. But when we separated the cerebellar samples into more bins, we were able to observe the expression of Purkinje neurons in a part of the association cerebellum (Figure S6). This supports emerging evidence of their role in cognitive functions, potentially linked to catecholamine signaling,[42,43] which is consistent with the high expression of monooxygenase- and oxidoreductase-related processes in the association cerebellum observed by GO GSVA, as they are both involved in the neurotransmission of catecholamines.[44]

In conclusion, the GSVA served to probe the possible intermediate molecular functions, cellular components, cell types, and biological processes that linked GCI_{sig} to the cerebellar SA axis. Thus, we were able to provide evidence of the possible biological principles of how GCI_{sig} scaffolds the SA axis, which is primarily by engaging neurotransmission and the Purkinje cells.

Cerebellar SA axis and its underlying genetic basis associated with multiple cerebellum-linked neuropsychiatric disorders

Prior evidence suggested that the dysfunction of the cerebellar functional organization plays a crucial role in various neurological[45,46] and psychiatric disorders,[9,47] many of which possess common underlying genetic risks.[48] In light of this, could the genetic basis underlying the cerebellar SA axis provide some evidence or new perspectives on the role of the cerebellum in brain disorders?

First, combining the GSVA with the disease gene network[49] enabled the visualization of changes in disease relevance along the cerebellar SA axis. Overall, more neurological disorders are associated with the sensorimotor cerebellum, but more psychiatric disorders are associated with the association cerebellum (Figure 3, purple box; Figure S7). This finding coincides with reports that showed that depression-relevant shifts in resting-state fMRI features were preferentially associated with heteromodal cortical areas compared to unimodal cortical areas.[50,51] Specifically, significant involvement of the association cerebellum in major affective disorder and Lewy body disease (Figure 3, purple box) was observed. Two main types of major affective disorder[52] are major depressive disorder (MDD) and bipolar disorder (BD), both of which have been linked to the cerebellum.[47] For example, a significant relationship between severe depressive symptoms and the cerebellar salience network has been observed in patients with MDD.[53] Dementia in patients with Lewy body disease showed gray matter loss in the posterior and lateral areas of the cerebellum, which belong to the association cerebellum.[54] In contrast, some neurological disorders that previously have been shown to relate to the cerebellum, such as amyotrophic lateral sclerosis (ALS), engage more in the sensorimotor cerebellum. A significantly increased FC of the cerebellum also has been observed in patients with ALS.[55]

Then, in relation to the *ex vivo* psychiatric gene dysfunction dataset[56] for five major psychiatric disorders (MDD, BD, autistic spectrum disorder [ASD], schizophrenia [SCZ], and alcohol abuse disorder [AAD]), we found that the GCI was significantly correlated with MDD, BD, ASD, and SCZ genetic dysfunction but not with AAD (Figures 4A and S8). Since MDD, BD, ASD, and SCZ are all characterized by mental disturbances, these findings are consistent with the significant engagement in the associated cerebellum of major affective disorder observed by the disease GSVA. This indicated that the GCI of the *in vivo* cerebellar SA axis from healthy Allen Human Brain Atlas (AHBA) subjects could capture gene dysregulation in *ex vivo* brain tissue from patients with cerebellum-linked psychiatric disorders,[51,57] one of which, i.e., SCZ, has been characterized by a compressed cerebellar FG.[9]

Combining the disease GSVA with an *ex vivo* psychiatric gene dysfunction analysis suggested that SA could be used as an imaging marker to investigate the cerebellar cross-disorder role and hinted at a possible convergence of SA alteration and gene dysfunction across multiple psychiatric disorders.

Developmental trajectory and evolution rate of GCI_{sig}

To give an overall temporal profile of GCI_{sig}, the GCI_{sig} could be clustered into 2 clusters (Figures 4C and S9), one of which was expressed more strongly before birth (n = 481) and was

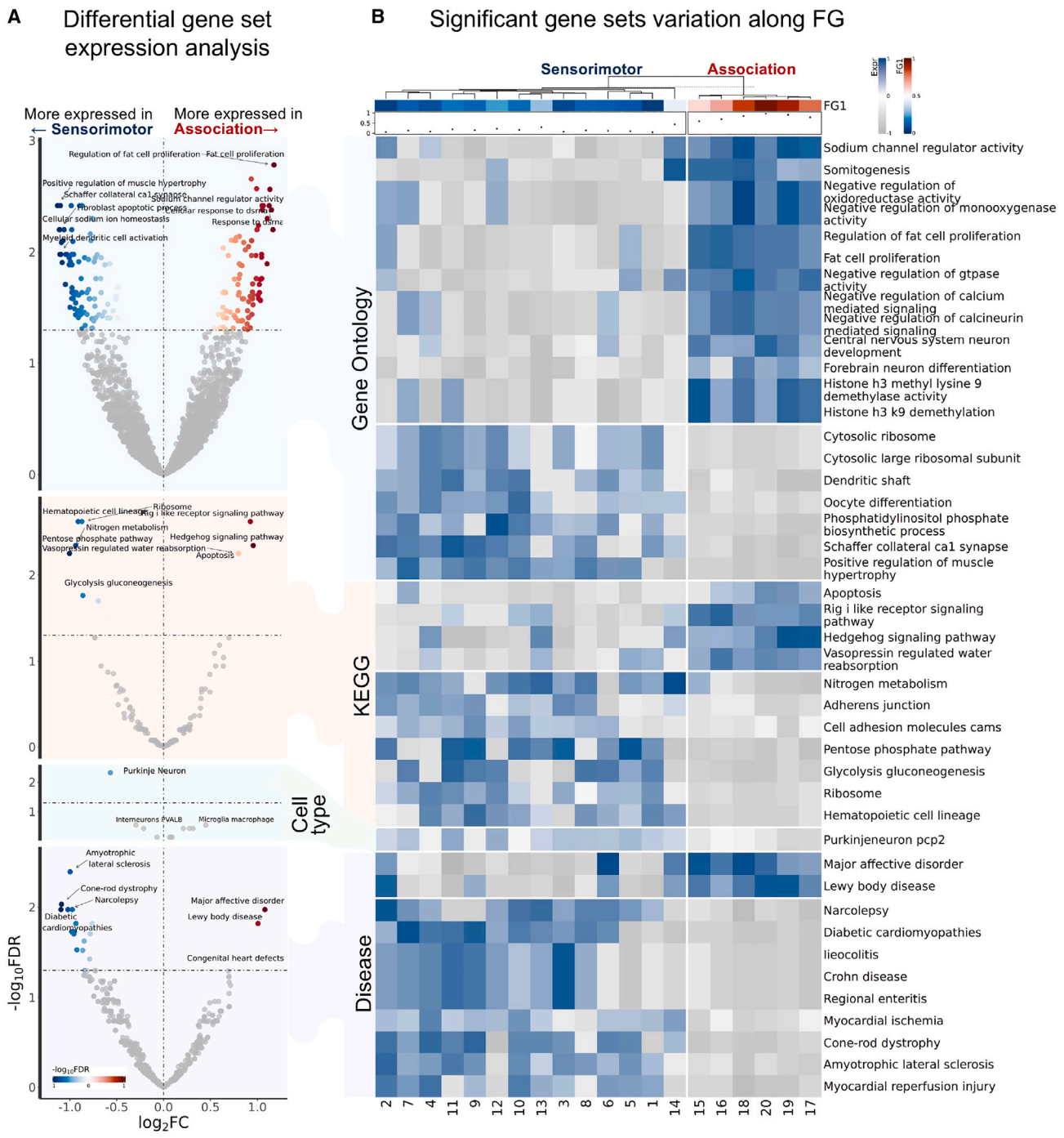

Figure 3. Surrogate intermediate biological principle scaffolding the SA axis

By leveraging the GSVA (Figure 1B left), the expression of GCI_{sig} along the SA axis was transformed into a gene set time bin matrix. The gene sets were separated into four categories: Gene Ontology (GO; blue), Kyoto Encyclopedia of Genes and Genomes (KEGG; orange), cell type (green), and disease (purple).

(A) Differential expression analysis examined each gene set and found significant changes between the sensorimotor (blue) and association regions (red) of the human cerebellum. Fold change >1 and $p < 0.05$ (false discovery rate [FDR] corrected) were used as indicators to threshold the significant gene sets.

(B) The heatmap shows the expression of the significant gene sets along the SA axis and the hierarchical clustering of the cerebellar sensorimotor and association bins. Note that the 20 bin-based analysis is presented here; other bin strategies can be found in Figures S4–S7. Full results can be found in Data S2–S9.

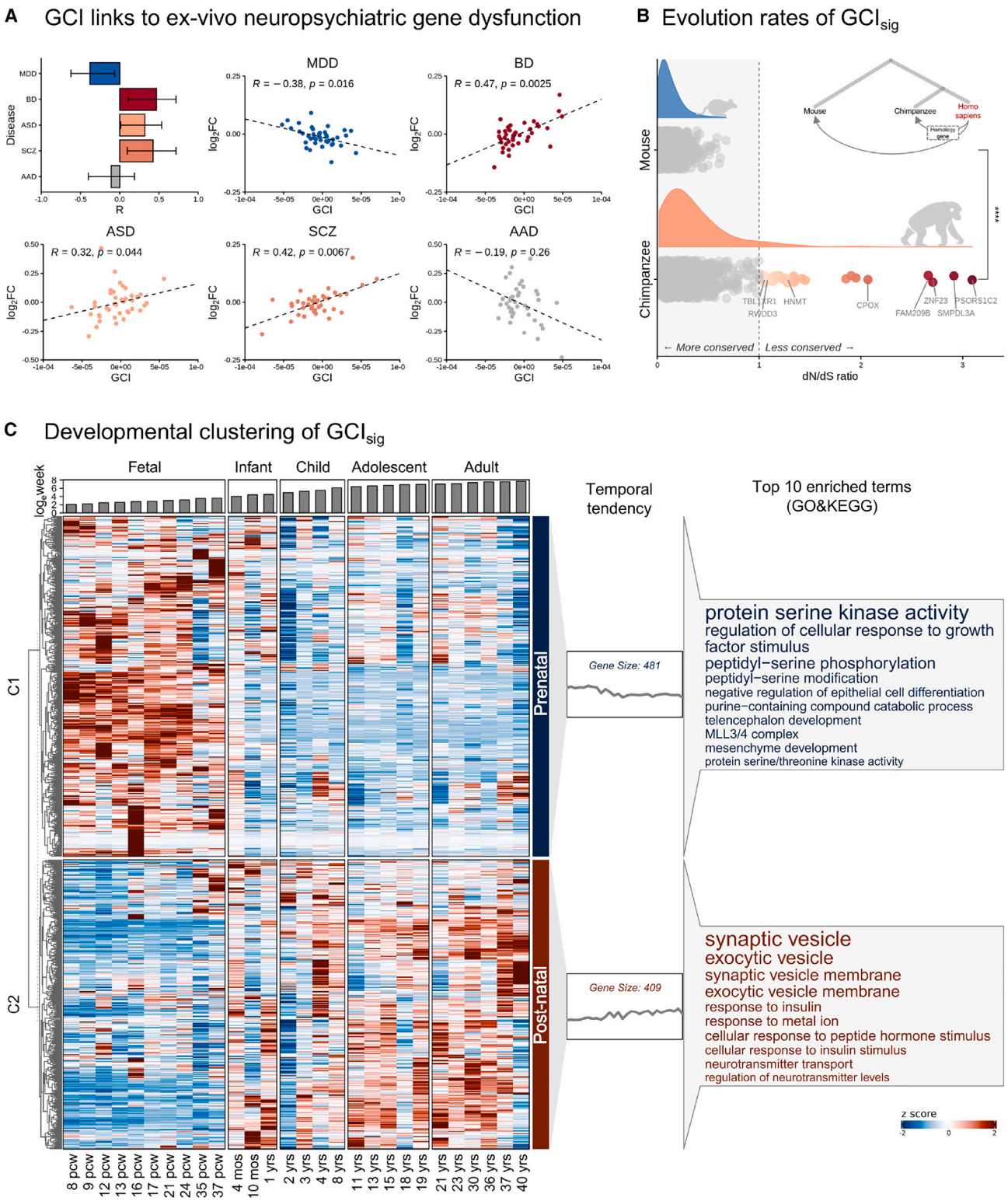

Figure 4. Neuropsychiatric gene dysfunction relatedness, development trajectory, and differential evolution rates with respect to mouse and chimpanzee

(A) Association between GCI and *ex vivo* gene dysregulation in major depression (MDD), bipolar disorder (BD), autistic spectrum disorder (ASD), schizophrenia (SCZ), and alcohol abuse disorder (AAD). The top left corner shows the correlation profiles for all the diseases. The height of the bar corresponds to the magnitude

(legend continued on next page)

correlated with protein serine kinase activity, regulation of cellular response to growth factor stimulus, and peptidyl-serine phosphorylation, all of which are involved in neurodevelopment-related processes. The other cluster had a greater expression after birth and was mainly associated with neurotransmission terms that are primarily linked to neuropsychiatric disorders.[58–60] These results reinforce findings of significant neurotransmission engagements in the association cerebellum and keep consistent with its prolonged development.[61] A more fine-grained clustering (Figure S9) also suggests that different clusters have distinct temporal tendencies and different enriched functions. In keeping with the consistency of the main results of the two clusters, they work together to remind us that the genetic basis of the cerebellar SA axis does not emerge suddenly but is formed gradually from fetal life to adulthood step by step, as different components act during different developmental windows.[62]

In addition to the ontogeny in the short period, we analyzed the evolutionary rate, i.e., *dN*/*dS*,[63] of GCI_{sig} to test whether the GCI_{sig} experienced positive selection (*dN*/*dS* > 1), neutral selection (*dN*/*dS* = 1), or negative selection (*dN*/*dS* < 1) in both the mouse-human and chimpanzee-human evolutionary processes. More *dN*/*dS* > 1 (n = 35) was observed in the chimpanzee-human evolution, whereas no *dN*/*dS* > 1 was observed in mouse-human evolution (Figure 4B). The difference was significant ($p < 0.0001$, mean comparison by Welch's t test). This implies that GCI_{sig} played a more crucial role in the evolution from chimpanzee to human. Moreover, several genes of the GCI_{sig} that was only positively selected during the evolution from chimpanzee to human, such as TBL1XR1, RWDD3, and HNMT,[64] were also linked to human accelerated regions (HARs).[65] This suggests that the genetic basis of the cerebellar SA axis in modern humans has been subjected to positive selection relatively recently in human evolution and that the cerebellar SA axis may have played a central part in the emergence of uniquely human cognitive abilities consistent with the extreme expansion of the human association cerebellum.[24,66]

Cerebello-cerebral interaction at genetic and connectivity levels

Given that the functional architecture of the human cerebellum has long been thought to be determined by extra-cerebellar connections,[1] it is interesting to speculate on how this principle of function acts on the SA axis and its spatio-molecular profiles.

First, by correlating the GCI_{sig} with the cerebral cortical sample-wise gene expression (n = 1,539), we created the cerebellar hierarchical representative index of similarity (CHRIS; Figure 5A, left top), a value representing the degree to which the genomic signature of the cerebellar SA axis is represented in the gene expression profile of a cerebral cortical sample. To discover the locations in the cerebral cortex that have a significant genetic correlation with the GCI_{sig}, which supports the cerebellar SA axis, a Bonferroni-corrected $p < (0.05/1{,}539)$ was utilized to identify the significant cerebral cortical samples (the set of these cerebral cortical samples with significant CHRIS was referred to as $CHRIS_{sig}$, n = 130; Figure 5A, left bottom). $CHRIS_{sig}^{-}$ (n = 15) and $CHRIS_{sig}^{+}$ (n = 115) indicate more significant similarity with the sensorimotor and association areas of the cerebellum, respectively. By plotting the $CHRIS_{sig}$ at the 7-network level (Figure 5A, right), $CHRIS_{sig}^{-}$ was found to be mainly located in the unimodal networks, that is, the visual, somatomotor, and dorsal attention networks, whereas $CHRIS_{sig}^{+}$ was mainly aggregated in the transmodal networks, that is, the default, control, ventral attention, and limbic networks. This indicates that GCI_{sig}, which supports the cerebellar SA axis, is genetically correlated with the cerebral cortex and that the genetic correlation pattern mirrors the cerebral cortical SA axis.[67,68]

Next, is it possible that $CHRIS_{sig}$ has significant connections with the cerebellum? $CHRIS_{sig}^{-}$ (Figure 5B, top left) and $CHRIS_{sig}^{+}$ (Figure 5B, bottom left) have a significant connection with the cerebellum, and their FCs are quite different. $CHRIS_{sig}^{-}$, which is significantly genetically correlated with the sensorimotor cerebellum, has a positive connection with the V, VI, and VIII lobules, which are aggregated in the somatomotor, ventral attention, and visual networks (Figure 5B, right blue circle). In contrast, $CHRIS_{sig}^{+}$, which is significantly genetically correlated with the association cerebellum, has a positive connection with the Crus I, Crus II, and IX lobules, which correspond to the limbic and default networks as well as with part of the control networks (Figure 5B, right red circle).

DISCUSSION

The goal of this study was to decode the spatio-molecular profiles underlying the cerebellar SA axis, which covers a wide range from genetic signatures, intermediate molecular patterns, cell types, and biological processes to cerebello-cerebral interactions. Along the cerebellar SA axis, there is increasing neurotransmission involvement, later maturation, more involvement in evolution, and increased susceptibility to psychiatric symptoms. The distinct intrinsic genetic variations deep within the microcircuit homogeneity genetically and functionally interact with those of the cerebral cortex as well as mirroring the SA axis of the human cerebral cortex and the cerebellum. Collectively, these findings hint at the possibility of SA axis formation at both the intrinsic progressive biological and cerebello-cerebral coordination levels and thus offer a springboard from which to synthesize multi-level findings into a general characterization of cerebellar function, as well as to go a step further to explore

of the correlation coefficient, indicating the strength and direction of the correlation with the disease phenotype. Error bars represent the 95% confidence intervals. In the following five scatter plots, the binned analysis revealed a negative relationship between the GCI of the cerebellar SA axis and gene downregulation in MDD and a positive association in BD, ASD, and SCZ, but not in AAD. Other bin strategies can be found in Figure S8.

(B) The horizontal violin plot overlay offers a density distribution of the *dN*/*dS* ratios, with blue representing mouse-human and orange representing chimpanzee-human, and the Wilcoxon test comparison between them indicating significant differences (Welch's t test $p < 0.0001$). Each dot shows each gene of GCI_{sig} and just the *dN*/*dS* > 1 (right of the vertical dashed line) colored according *dN*/*dS* magnitude.

(C) Utilizing the Mfuzz clustering method in GCI_{sig}, development expression classified GCI_{sig} into 2 clusters (left). The choice of the optimal cluster number can be found in Figure S9. Each cluster has a distinct temporal trajectory (middle) and biological function (right).

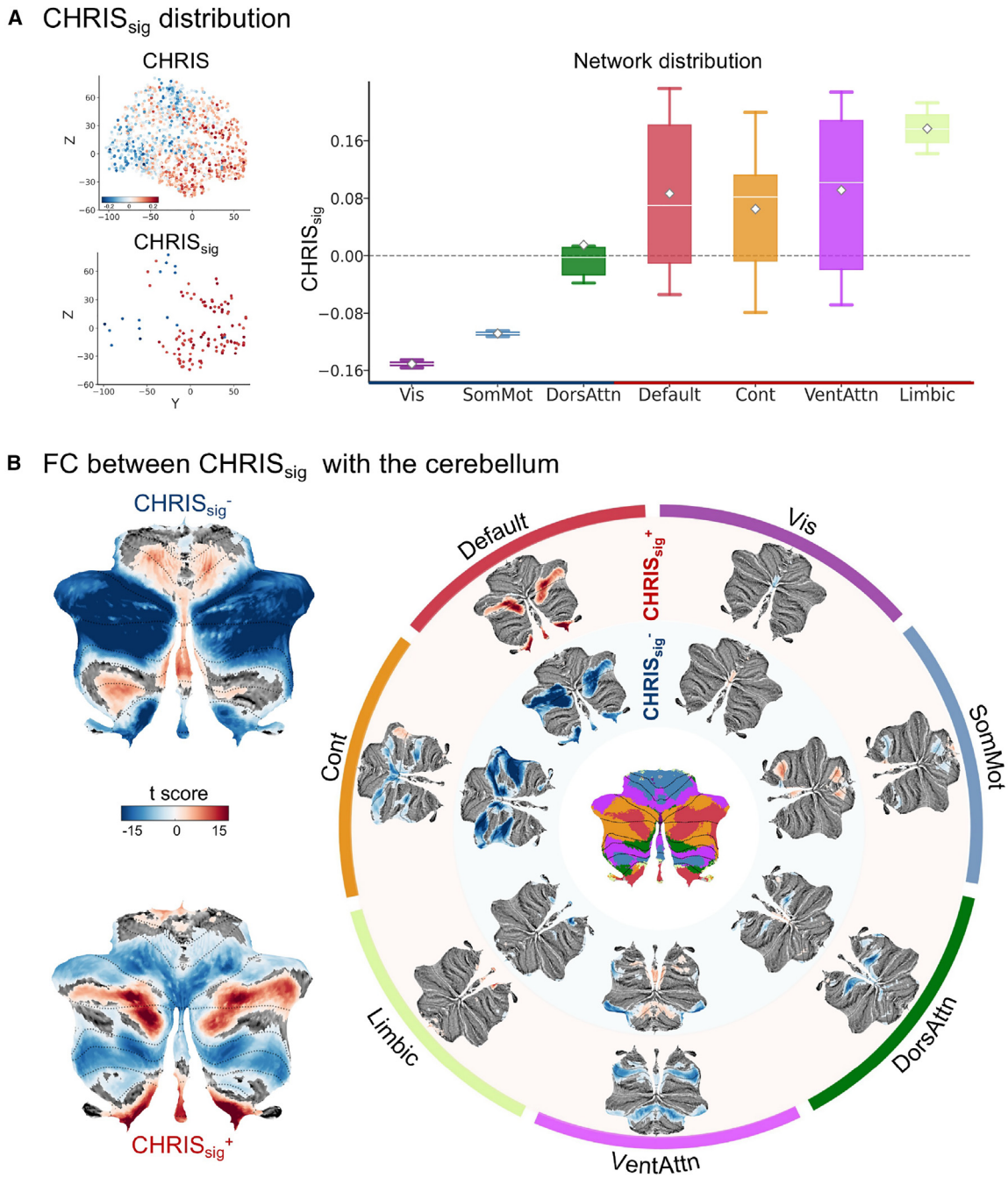

Figure 5. The CHRIS$_{sig}$ distribution and its FC with the cerebellum

(A) By correlating the GCI$_{sig}$ with the gene expression of the cerebral cortex, we obtained the CHRIS (top left), which represents the genetic interaction between the cerebral cortex and the gene substrates underlying the cerebellar SA axis, i.e., GCI$_{sig}$. CHRIS$_{sig}$ (bottom left) was evaluated by Bonferroni correction with a correlation significance $p < (0.05/1{,}539)$ and represents the set of cerebral cortical samples with significant CHRIS. The distribution of CHRIS$_{sig}$ across 7 networks (right) is shown by a boxplot ordered by the median value at the bottom (the mean is represented by a diamond marker with a white face and gray edge, while the median is depicted by a white line; the whiskers, which illustrate the range of the data, are presented with a thicker line width).

(B) The FC between the CHRIS$_{sig}^+$ (top left) and CHRIS$_{sig}^-$ (bottom left) and the human cerebellum was largely different, as was the distribution of FC across the networks (right).

the underestimated contribution of the cerebellar SA axis to human functions along with its role in neuropsychiatric disorders and brain evolution.

Shaping of the cerebellar SA axis

The SA axis has long been identified in the cerebral cortex and was found to be extensively associated with various features

derived from different modalities.[4] But how the cerebellar SA axis is established remains unexplored. We approached this question from two main perspectives: are there possible intrinsic subtle genetic variations deep within the high microcircuit homogeneity, which have been demonstrated in animal cerebella, and how do those relate to the widely accepted connections between the cerebellum and the cerebral cortex?

Recent animal discoveries have suggested that cerebellar histology is not entirely uniform or homogeneous.[2] Does the human cerebellum, previously believed to be characterized by a uniform cytoarchitecture, also exhibit diverse compartments with specialized cellular, molecular, and synaptic properties for different functions, as observed in animal models?[69,70] In this study, we decoded the genetic, cellular, and biological processes of the human cerebellar SA axis by introducing GSVA into imaging-transcriptomic studies with the goal of describing how the SA axis progresses at spatio-molecular level. Significantly differently expressed gene sets were able to differentiate sensorimotor and association areas of the cerebellum. This suggests that the cerebellum seems to be more intrinsically microscopically varied along the SA axis than traditionally thought, so the biological configuration of the human cerebellum is not entirely uniform or homogeneous if explored in more elaborate detail.[2,61,70]

Meanwhile, the differences in Purkinje cells along the SA axis were not very significant. Note that the results that we found do not mean that Purkinje cells are not expressed in the association cerebellum. Combined with the observed expression of Purkinje cells in the association cerebellum when considering more bins (Figure S6), our results only suggest that genes associated with Purkinje cells, as defined by the chosen cell-type set (DropViz[36]), show differences in expression between the sensorimotor and association areas of the cerebellum. Purkinje cells are the sole source of output from the human cerebellum, and the most well-studied zebrin regions defined by the two subtypes of Purkinje cells in animal models separately correspond to motor and non-motor functions.[22] Therefore, the significantly different expression of Purkinje cells now observed between the sensorimotor and associative cerebellum is likely related to the formation of the human cerebellar SA axis. The molecular variation within cerebellar cell type was more continuous rather than discrete,[21] so if future techniques can define the finer cell types of the human cerebellum more specifically, then they could provide more detailed answers. Nevertheless, the present results of the optimal combination of current databases and methods remind us that the Purkinje cells are involved in the organization of the cerebellar SA axis and suggest that the cellular architecture is not strictly homogeneous if the cells are subtyped, especially with respect to the zebrin differentiated subtypes of Purkinje cells.[70]

In addition to the general summary these results provide, it may also be very interesting to carefully dig into the detailed biological principles that correlate specifically with the SA axis and thus might support it. Some of these microscopic biological principles have been studied on multiple scales and found to have relatively direct relationships with cerebellar function and dysfunction in diseases, including involvements in neurotransmissions,[71] ribosomes,[39] and dendritic shafts.[40] For example, more neurotransmission processes are expressed higher in the association cerebellum than in the sensorimotor cerebellum, which might explain how the association cerebellum has a characteristic diverse functional profile[71] and, further, why the association cerebellum is correlated with many neuropsychiatric disorders, which are characterized by cognitive and emotional impairments as well as dysfunction in neurotransmission.[58–60] Besides, there is a large proportion of processes whose links to cerebellar functional organization (e.g., fat cell proliferation) remain unclear and require continued future exploration.

To address the question of how the cerebellar SA axis is formed, in addition to the intrinsic microstructural features we discussed above, another contribution that cannot be ignored and has been widely studied is the connection to the cerebral cortex.[1] Although extra-cerebellar connections have been implicated in the functional differentiation of the human cerebellum,[1,10] it is unclear whether the cerebellar SA axis is formed through a mirrored projection of the cerebral cortical SA axis. When we projected the gene-SA relationship of the human cerebellum, i.e., the GCI_{sig} of the cerebellar SA axis, to the cerebral cortex, we found that the distribution of this projection ($CHRIS_{sig}$) mirrors the SA axis along the cerebral cortex.[4] In addition, the significant cerebral cortical locations, i.e., $CHRIS_{sig}^{-}$ and $CHRIS_{sig}^{+}$, which are, respectively, genetically similar to those of the sensorimotor and association areas of the cerebellum, also have distinct significant FC with the cerebellum. These findings demonstrate that the interaction between the cerebellum and cerebral cortex might be involved in the formation of the cerebellar SA axis[7] and provide evidence for a new perspective on the unifying SA axis of the whole brain[4] and especially for the gradient correspondence between the cerebral cortex and cerebellum.[10]

In summary, our results probed the biological basis of cerebellar SA axis formation at two levels, including the intrinsic microscopic characterization of molecular, cellular, and pathway variations along the cerebellar SA axis, as well as the cerebral cortical interaction to the cerebellum at both the genetic and functional levels. The genetic and functional cerebello-cerebral interactions evaluated based on these intrinsic microscopic variations, respectively, mirror the SA axis of the human cerebral cortex and the cerebellum. Therefore, they are not mutually exclusive but complementary in the formation of the cerebellar SA axis, which keeps consistent with the recent evidence that challenges the notion that the hierarchical structure of the human cerebellum is solely driven by cerebral cortex signals.

Convergence of development- and evolution-conferred psychiatric susceptibility in the association cerebellum

Decoding how the cerebellar SA axis is formed may yield deep insights into the vital roles of the cerebellum, such as in neuropsychiatric dysregulation and evolution. The rare perspective of variation along one axis represented by the FG offers a springboard for synthesizing multi-level findings into a general characterization of cerebellar function. Along the cerebellar SA axis, the sensorimotor cerebellum, which is mainly connected to the cerebral cortical motor regions and plays a role in motor function,[72] exhibits a relatively high expression of Purkinje neurons, is enriched in multiple levels of fundamental biological processes,

and engages in many cerebellum-linked neurological disorders. In contrast, the association cerebellum, which is primarily connected to the association regions of the cerebral cortex and in charge of the non-motor functions such as emotion and cognition,[72] is enriched in many neurotransmission processes, undergoes delayed maturation,[61] is involved in many psychiatric disorders, and has rapidly expanded in recent human evolution.[66] Furthermore, the present findings with respect to neuropsychiatric disorders, neurodevelopment, and human evolution are mutually supportive and thus hint at the convergence of susceptibility to psychiatric symptoms conveyed by both neurodevelopment and recent rapid evolution in the association cerebellum.

The spatio-molecular profiles underlying the cerebellar SA axis derived from healthy subjects is significantly correlated with gene dysfunction in patients with SCZ, MDD, BD, and ASD. This finding resonated with the accumulated knowledge about the crucial role of the human cerebellum across psychiatric disorders and common underlying genetic risk sharing between these heritable psychiatric disorders.[48] Moreover, the engagement of GCI_{sig} in these psychiatric disorders is much more significant in the association cerebellum than in the sensorimotor cerebellum. Because these psychiatric disorders all involve dysregulation of emotional cognition in terms of symptoms and neurotransmission in terms of pathogenesis,[59,60] this is not only in harmony with the functional hierarchical nature along the cerebellar SA axis but is also consistent with the higher enrichment of neurotransmission in the association cerebellum. Several neurological disorders involving the sensorimotor cerebellum, such as ALS,[73,74] also manifest some psychological symptoms. Although there is a growing body of research on the cerebellum across brain disorders, the actual mechanisms are unclear.[47,75] The present results remind us that the sensorimotor and association areas of the cerebellum may not be strictly distinguished as, respectively, involved in neurological and psychiatric disorders but rather exhibit symptomatic changes along the SA axis, from the sensorimotor cerebellum to the association cerebellum, with more psychiatric symptoms that affect emotional or/and cognitive functions being involved. That is, along the cerebellar SA axis, there is increased susceptibility to psychiatric symptoms.[4]

On the one hand, in the cerebral cortex, the SA axis can be viewed as both a dominant spatial feature axis and a primary neurodevelopmental axis, implying that the variability of the spatial features may be partially derived from the variability of the development.[4] The developmental critical period progressed sequentially along the cerebral cortical SA axis. In a bifurcated manner, the sensorimotor cortex is refined in childhood, whereas the association cortex continues to mature throughout adolescence.[62] This is consistent with our transcriptomic-derived developmental findings that the postnatal cluster of GCI_{sig} is enriched in neurotransmission and aligns with increased psychiatric susceptibility in the association cerebellum. The association cerebellum is characterized by prolonged development,[61] and increased neurotransmission facilitates its continued plasticity.[76] One of its manifestations is that transmodal association regions remain comparatively immature throughout childhood and adolescence,[4,62] and thus the same damage in these time periods leads to more profound psychiatric symptoms.[77] For example, the high-risk time window for MDD is between the ages of 18 and 29[78] and for ASD is from infancy to childhood.[79] These findings suggest that the long-term plasticity within the later-maturing association cerebellum, which is involved in neurotransmission, conveys a psychiatric risk similar to that of the cerebral cortex.[4] More detailed, 8-cluster results indicate that gene sets with different functions exhibit temporal variation in their activity during the development process (fetal to adult). As such, it appears that, in the same way as the cerebral cortex, the hierarchical development along the SA axis is driven by a cascade of critical periods.[62,80,81] Future detailed developmental gene datasets within the human cerebellum would provide more inspiration.

On the other hand, from an evolutionary perspective, we found that the GCI_{sig} was positively selected during evolution from chimpanzee to human and linked to the HARs. This supports the idea that the cerebellar SA axis and its spatio-molecular profiles have played a crucial role in human evolution, especially the presence of unique human higher-order functions in recent evolution. This is consistent with the extreme selective expansion of the human association cerebellum.[24,66] Moreover, many positively selected genes are related to neuropsychiatric disorders, a finding that is consistent with the significant correlation between GCI and psychiatric genetic dysregulation. Taking the top *dN/dS* gene as an example, the PSORS1C2 gene as well as SMPDL3A were found to be linked with depression and SCZ[82] by regulating sphingomyelin metabolism.[83] This result supports present findings of the close relationship between GCI_{sig} and neuropsychiatric disorders and may also help in understanding why evolutionary changes are specific to the association cerebellum.[66] Furthermore, the hypothesis that increased susceptibility to mental illness may have accompanied the evolution of higher-order functions in the cerebral cortex is again implied at the cerebellum level.[84]

In summary, along the cerebellar SA axis, there is increasing neurotransmission involvement, later maturation, more involvement in evolution, and increased susceptibility to psychiatric symptoms. Because a combination of these with a close relationship between features derived from the cerebral cortex,[4] such as the protracted maturation of the association cortex, could significantly distinguish humans from other primates,[85] we infer that neurodevelopmental and evolutionary concomitant psychiatric susceptibility converges at the association cerebellum.

Limitations of the study

Several methodological limitations need to be noted when interpreting our findings, and these limitations suggest important avenues for future research. First, we could not replicate our results using an external gene dataset because there is currently no publicly accessible dataset that is comparable to AHBA, which provides a comprehensive sampling of the human cerebellum.[30] We have tried to address this problem by regressing donor effects in the genetic data preprocessing step and performing a leave-one-out donor analysis. Second, when we tried to use GSVA to obtain a significant gene set along the SA axis, we divided the SA axis into the sensorimotor and association areas

of the cerebellum. However, there are other functional variants between these two termini. So, while this is also why this work can provide a fresh perspective, there should still be more enhancements and more detailed discussions in the future. Third, although current work overcomes one of the issues of imaging transcriptomics by introducing GSVA, it is still very challenging to make causal inferences.

In short, more detailed cerebellar genetic datasets and more advanced methods are necessary to answer deeper questions in a causal rather than a correlational manner. Nevertheless, given the current limited understanding of how microscale genes contribute to cerebellar functional diversity, this study presents fresh insights into the genetic, molecular, cellular, and pathway variations and cerebello-cerebral interactions that appear to scaffold the human cerebellar SA axis. This fresh perspective is attributable to our introduction of GSVA into imaging transcriptomics and analysis along the continuous SA axis. Such an analysis is not available for discrete functional networks or with traditional imaging-transcriptomics techniques.[30] So, while there are several limitations in the dataset and methodology of the current work, this methodological advancement can still provide valuable results.

STAR★METHODS

Detailed methods are provided in the online version of this paper and include the following:

- KEY RESOURCES TABLE
- RESOURCE AVAILABILITY
  - Lead contact
  - Materials availability
  - Data and code availability
- METHOD DETAILS
  - Experimental design
  - The FG of the human cerebellum
  - Human transcriptome data
  - Prediction of FG using the transcriptome
  - Gene set variation analysis (GSVA)
  - Relationships with neuropsychiatric disorders
  - Developmental clustering and evolution rate
  - Cerebral cortical interaction with GCI_{sig}
- QUANTIFICATION AND STATISTICAL ANALYSIS

SUPPLEMENTAL INFORMATION

Supplemental information can be found online at https://doi.org/10.1016/j.celrep.2024.113770.

ACKNOWLEDGMENTS

This work was supported by the STI2030-Major Projects (grant no. 2021ZD0200203 to L.F.) and the Natural Science Foundation of China (grant nos. 82072099 to L.F. and 62250058 to C.C.). The authors appreciate the English language and editing assistance provided by Rhoda E. and Edmund F. Perozzi, PhDs. Data were provided by the Human Connectome Project, WU-Minn Consortium (principal investigators: David Van Essen and Kamil Ugurbil; 1U54MH091657) funded by the 16 NIH Institutes and Centers that support the NIH Blueprint for Neuroscience Research, and by the McDonnell Center for Systems Neuroscience at Washington University.

AUTHOR CONTRIBUTIONS

Yaping Wang, K.H.M., C.C., and L.F. designed the research; Yaping Wang performed the experiments; Yaping Wang, Yufan Wang, H.W., L.M., K.H.M., L.F., and C.C. contributed new analytic tools; Yaping Wang analyzed the data; Yaping Wang, K.H.M., C.C., and L.F. wrote the paper; and L.F., C.C., S.B.E., and K.H.M. contributed analytical expertise, theoretical guidance, paper revisions, and informed interpretation of the results.

DECLARATION OF INTERESTS

The authors declare no competing interests.

Received: September 26, 2023
Revised: December 27, 2023
Accepted: January 25, 2024

REFERENCES

1. Schmahmann, J.D., Guell, X., Stoodley, C.J., and Halko, M.A. (2019). The theory and neuroscience of cerebellar cognition. Annu. Rev. Neurosci. *42*, 337–364. https://doi.org/10.1146/annurev-neuro-070918-050258.
2. De Zeeuw, C.I., Lisberger, S.G., and Raymond, J.L. (2021). Diversity and dynamism in the cerebellum. Nat. Neurosci. *24*, 160–167. https://doi.org/10.1038/s41593-020-00754-9.
3. Guell, X., and Schmahmann, J.D. (2023). Fmri-based anatomy: Mapping the cerebellum. In Essentials of Cerebellum and Cerebellar Disorders: A Primer for Graduate Students, D.L. Gruol, N. Koibuchi, M. Manto, M. Molinari, J.D. Schmahmann, and Y. Shen, eds. (Springer International Publishing), pp. 351–356. https://doi.org/10.1007/978-3-031-15070-8_54.
4. Sydnor, V.J., Larsen, B., Bassett, D.S., Alexander-Bloch, A., Fair, D.A., Liston, C., Mackey, A.P., Milham, M.P., Pines, A., Roalf, D.R., et al. (2021). Neurodevelopment of the association cortices: Patterns, mechanisms, and implications for psychopathology. Neuron *109*, 2820–2846. https://doi.org/10.1016/j.neuron.2021.06.016.
5. Guell, X. (2022). Functional gradients of the cerebellum: A review of practical applications. Cerebellum *21*, 1061–1072. https://doi.org/10.1007/s12311-021-01342-8.
6. Habas, C. (2021). Functional connectivity of the cognitive cerebellum. Front. Syst. Neurosci. *15*, 642225. https://doi.org/10.3389/fnsys.2021.642225.
7. Guell, X., Schmahmann, J.D., Gabrieli, J.D., and Ghosh, S.S. (2018). Functional gradients of the cerebellum. Elife *7*, e36652. https://doi.org/10.7554/eLife.36652.
8. D'Mello, A.M., Gabrieli, J.D.E., and Nee, D.E. (2020). Evidence for hierarchical cognitive control in the human cerebellum. Curr. Biol. *30*, 1881–1892.e3. https://doi.org/10.1016/j.cub.2020.03.028.
9. Dong, D., Luo, C., Guell, X., Wang, Y., He, H., Duan, M., Eickhoff, S.B., and Yao, D. (2020). Compression of cerebellar functional gradients in schizophrenia. Schizophr. Bull. *46*, 1282–1295. https://doi.org/10.1093/schbul/sbaa016.
10. Katsumi, Y., Zhang, J., Chen, D., Kamona, N., Bunce, J.G., Hutchinson, J.B., Yarossi, M., Tunik, E., Dickerson, B.C., Quigley, K.S., and Barrett, L.F. (2023). Correspondence of functional connectivity gradients across human isocortex, cerebellum, and hippocampus. Commun. Biol. *6*, 401. https://doi.org/10.1038/s42003-023-04796-0.
11. Strick, P.L., Dum, R.P., and Fiez, J.A. (2009). Cerebellum and nonmotor function. Annu. Rev. Neurosci. *32*, 413–434. https://doi.org/10.1146/annurev.neuro.31.060407.125606.
12. Schmahmann, J.D., and Pandya, D.N. (1997). The cerebrocerebellar system. Int. Rev. Neurobiol. *41*, 31–60. https://doi.org/10.1016/s0074-7742(08)60346-3.

13. Schmahmann, J.D. (1996). From movement to thought: Anatomic substrates of the cerebellar contribution to cognitive processing. Hum. Brain Mapp. *4*, 174–198. https://doi.org/10.1002/(sici)1097-0193(1996)4:3<174::Aid-hbm3>3.0.Co;2-0.

14. Hoshi, E., Tremblay, L., Féger, J., Carras, P.L., and Strick, P.L. (2005). The cerebellum communicates with the basal ganglia. Nat. Neurosci. *8*, 1491–1493. https://doi.org/10.1038/nn1544.

15. Kelly, R.M., and Strick, P.L. (2003). Cerebellar loops with motor cortex and prefrontal cortex of a nonhuman primate. J. Neurosci. *23*, 8432–8444. https://doi.org/10.1523/JNEUROSCI.23-23-08432.2003.

16. Akkal, D., Dum, R.P., and Strick, P.L. (2007). Supplementary motor area and presupplementary motor area: Targets of basal ganglia and cerebellar output. J. Neurosci. *27*, 10659–10673. https://doi.org/10.1523/JNEUROSCI.3134-07.2007.

17. Coffman, K.A., Dum, R.P., and Strick, P.L. (2011). Cerebellar vermis is a target of projections from the motor areas in the cerebral cortex. Proc. Natl. Acad. Sci. USA *108*, 16068–16073. https://doi.org/10.1073/pnas.1107904108.

18. Middleton, F.A., and Strick, P.L. (2001). Cerebellar projections to the prefrontal cortex of the primate. J. Neurosci. *21*, 700–712. https://doi.org/10.1523/JNEUROSCI.21-02-00700.2001.

19. Voogd, J. (2014). What we do not know about cerebellar systems neuroscience. Front. Syst. Neurosci. *8*, 227. https://doi.org/10.3389/fnsys.2014.00227.

20. Zhou, H., Lin, Z., Voges, K., Ju, C., Gao, Z., Bosman, L.W.J., Ruigrok, T.J.H., Hoebeek, F.E., De Zeeuw, C.I., and Schonewille, M. (2014). Cerebellar modules operate at different frequencies. Elife *3*, e02536. https://doi.org/10.7554/eLife.02536.

21. Kozareva, V., Martin, C., Osorno, T., Rudolph, S., Guo, C., Vanderburg, C., Nadaf, N., Regev, A., Regehr, W.G., and Macosko, E. (2021). A transcriptomic atlas of mouse cerebellar cortex comprehensively defines cell types. Nature *598*, 214–219. https://doi.org/10.1038/s41586-021-03220-z.

22. Lin, Y.C., Hsu, C.C.H., Wang, P.N., Lin, C.P., and Chang, L.H. (2020). The relationship between zebrin expression and cerebellar functions: Insights from neuroimaging studies. Front. Neurol. *11*, 315. https://doi.org/10.3389/fneur.2020.00315.

23. Haldipur, P., Aldinger, K.A., Bernardo, S., Deng, M., Timms, A.E., Overman, L.M., Winter, C., Lisgo, S.N., Razavi, F., Silvestri, E., et al. (2019). Spatiotemporal expansion of primary progenitor zones in the developing human cerebellum. Science *366*, 454–460. https://doi.org/10.1126/science.aax7526.

24. Barton, R.A., and Venditti, C. (2014). Rapid evolution of the cerebellum in humans and other great apes. Curr. Biol. *24*, 2440–2444. https://doi.org/10.1016/j.cub.2014.08.056.

25. Arnatkeviciute, A., Fulcher, B.D., and Fornito, A. (2019). A practical guide to linking brain-wide gene expression and neuroimaging data. Neuroimage *189*, 353–367. https://doi.org/10.1016/j.neuroimage.2019.01.011.

26. Richiardi, J., Altmann, A., Milazzo, A.C., Chang, C., Chakravarty, M.M., Banaschewski, T., Barker, G.J., Bokde, A.L.W., Bromberg, U., Büchel, C., et al. (2015). Brain networks. Correlated gene expression supports synchronous activity in brain networks. Science *348*, 1241–1244. https://doi.org/10.1126/science.1255905.

27. Anderson, K.M., Krienen, F.M., Choi, E.Y., Reinen, J.M., Yeo, B.T.T., and Holmes, A.J. (2018). Gene expression links functional networks across cortex and striatum. Nat. Commun. *9*, 1428. https://doi.org/10.1038/s41467-018-03811-x.

28. Hawrylycz, M.J., Lein, E.S., Guillozet-Bongaarts, A.L., Shen, E.H., Ng, L., Miller, J.A., van de Lagemaat, L.N., Smith, K.A., Ebbert, A., Riley, Z.L., et al. (2012). An anatomically comprehensive atlas of the adult human brain transcriptome. Nature *489*, 391–399. https://doi.org/10.1038/nature11405.

29. Fornito, A., Arnatkevičiūtė, A., and Fulcher, B.D. (2019). Bridging the gap between connectome and transcriptome. Trends Cogn. Sci. *23*, 34–50. https://doi.org/10.1016/j.tics.2018.10.005.

30. Wang, Y., Chai, L., Chu, C., Li, D., Gao, C., Wu, X., Yang, Z., Zhang, Y., Xu, J., Nyengaard, J.R., et al. (2022). Uncovering the genetic profiles underlying the intrinsic organization of the human cerebellum. Mol. Psychiatry *27*, 2619–2634. https://doi.org/10.1038/s41380-022-01489-8.

31. Hänzelmann, S., Castelo, R., and Guinney, J. (2013). Gsva: Gene set variation analysis for microarray and rna-seq data. BMC Bioinf. *14*, 7. https://doi.org/10.1186/1471-2105-14-7.

32. King, M., Hernandez-Castillo, C.R., Poldrack, R.A., Ivry, R.B., and Diedrichsen, J. (2019). Functional boundaries in the human cerebellum revealed by a multi-domain task battery. Nat. Neurosci. *22*, 1371–1378. https://doi.org/10.1038/s41593-019-0436-x.

33. Ashburner, M., Ball, C.A., Blake, J.A., Botstein, D., Butler, H., Cherry, J.M., Davis, A.P., Dolinski, K., Dwight, S.S., Eppig, J.T., et al. (2000). Gene ontology: Tool for the unification of biology. The gene ontology consortium. Nat. Genet. *25*, 25–29. https://doi.org/10.1038/75556.

34. Harris, M.A., Clark, J., Ireland, A., Lomax, J., Ashburner, M., Foulger, R., Eilbeck, K., Lewis, S., Marshall, B., Mungall, C., et al. (2004). The gene ontology (go) database and informatics resource. Nucleic Acids Res. *32*, D258–D261. https://doi.org/10.1093/nar/gkh036.

35. Kanehisa, M., Goto, S., Kawashima, S., Okuno, Y., and Hattori, M. (2004). The kegg resource for deciphering the genome. Nucleic Acids Res. *32*, D277–D280. https://doi.org/10.1093/nar/gkh063.

36. Saunders, A., Macosko, E.Z., Wysoker, A., Goldman, M., Krienen, F.M., de Rivera, H., Bien, E., Baum, M., Bortolin, L., Wang, S., et al. (2018). Molecular diversity and specializations among the cells of the adult mouse brain. Cell *174*, 1015–1030.e16. https://doi.org/10.1016/j.cell.2018.07.028.

37. Augustine, G.J., Santamaria, F., and Tanaka, K. (2003). Local calcium signaling in neurons. Neuron *40*, 331–346. https://doi.org/10.1016/S0896-6273(03)00639-1.

38. Yao, P.J., Petralia, R.S., and Mattson, M.P. (2016). Sonic hedgehog signaling and hippocampal neuroplasticity. Trends Neurosci. *39*, 840–850. https://doi.org/10.1016/j.tins.2016.10.001.

39. Kawaguchi, S.Y., and Hirano, T. (2013). Gating of long-term depression by ca2+/calmodulin-dependent protein kinase ii through enhanced cgmp signalling in cerebellar purkinje cells. J. Physiol. *591*, 1707–1730. https://doi.org/10.1113/jphysiol.2012.245787.

40. Lee, K.J., Kim, H., and Rhyu, I.J. (2005). The roles of dendritic spine shapes in purkinje cells. Cerebellum *4*, 97–104. https://doi.org/10.1080/14734220510007842.

41. Ito, M. (2002). Historical review of the significance of the cerebellum and the role of purkinje cells in motor learning. Ann. N. Y. Acad. Sci. *978*, 273–288. https://doi.org/10.1111/j.1749-6632.2002.tb07574.x.

42. Locke, T.M., Fujita, H., Hunker, A., Johanson, S.S., Darvas, M., du Lac, S., Zweifel, L.S., and Carlson, E.S. (2020). Purkinje cell-specific knockout of tyrosine hydroxylase impairs cognitive behaviors. Front. Cell. Neurosci. *14*, 228. https://doi.org/10.3389/fncel.2020.00228.

43. Chaudhari, K., Wang, L., Kruse, J., Winters, A., Sumien, N., Shetty, R., Prah, J., Liu, R., Shi, J., Forster, M., and Yang, S.H. (2021). Early loss of cerebellar purkinje cells in human and a transgenic mouse model of alzheimer's disease. Neurol. Res. *43*, 570–581. https://doi.org/10.1080/01616412.2021.1893566.

44. Nagatsu, T. (2007). The catecholamine system in health and disease—relation to tyrosine 3-monooxygenase and other catecholamine-synthesizing enzymes. Proc. Jpn. Acad., Ser. B *82*, 388–415.

45. Schmahmann, J.D. (2004). Disorders of the cerebellum: Ataxia, dysmetria of thought, and the cerebellar cognitive affective syndrome. J. Neuropsychiatry Clin. Neurosci. *16*, 367–378. https://doi.org/10.1176/jnp.16.3.367.

46. Diwakar, S. (2017). Cerebellum in neurological disorders: A review on the role of inter-connected neural circuits. J. neurol. stroke *6*. https://doi.org/10.15406/jnsk.2017.06.00196.

47. Phillips, J.R., Hewedi, D.H., Eissa, A.M., and Moustafa, A.A. (2015). The cerebellum and psychiatric disorders. Front. Public Health *3*, 66. https://doi.org/10.3389/fpubh.2015.00066.

48. Brainstorm Consortium; Anttila, V., Bulik-Sullivan, B., Finucane, H.K., Walters, R.K., Bras, J., Duncan, L., Escott-Price, V., Falcone, G.J., Gormley, P., et al. (2018). Analysis of shared heritability in common disorders of the brain. Science *360*, eaap8757. https://doi.org/10.1126/science.aap8757.

49. Piñero, J., Ramírez-Anguita, J.M., Saüch-Pitarch, J., Ronzano, F., Centeno, E., Sanz, F., and Furlong, L.I. (2020). The disgenet knowledge platform for disease genomics: 2019 update. Nucleic Acids Res. *48*, D845–D855. https://doi.org/10.1093/nar/gkz1021.

50. Cole, M.W., Repovš, G., and Anticevic, A. (2014). The frontoparietal control system: A central role in mental health. Neuroscientist *20*, 652–664. https://doi.org/10.1177/1073858414525995.

51. Anderson, K.M., Collins, M.A., Kong, R., Fang, K., Li, J., He, T., Chekroud, A.M., Yeo, B.T.T., and Holmes, A.J. (2020). Convergent molecular, cellular, and cortical neuroimaging signatures of major depressive disorder. Proc. Natl. Acad. Sci. USA *117*, 25138–25149. https://doi.org/10.1073/pnas.2008004117.

52. Ellenbroek, B., and Youn, J. (2016). Chapter 7 - affective disorders. In Gene-environment Interactions in Psychiatry, B. Ellenbroek and J. Youn, eds. (Academic Press), pp. 173–231. https://doi.org/10.1016/B978-0-12-801657-2.00007-0.

53. Bogoian, H.R., King, T.Z., Turner, J.A., Semmel, E.S., and Dotson, V.M. (2020). Linking depressive symptom dimensions to cerebellar subregion volumes in later life. Transl. Psychiatry *10*, 201. https://doi.org/10.1038/s41398-020-00883-6.

54. Colloby, S.J., O'Brien, J.T., and Taylor, J.P. (2014). Patterns of cerebellar volume loss in dementia with lewy bodies and alzheimer's disease: A vbm-dartel study. Psychiatry Res. *223*, 187–191. https://doi.org/10.1016/j.pscychresns.2014.06.006.

55. Prell, T., and Grosskreutz, J. (2013). The involvement of the cerebellum in amyotrophic lateral sclerosis. Amyotroph Lat Scl Fr *14*, 507–515. https://doi.org/10.3109/21678421.2013.812661.

56. Gandal, M.J., Haney, J.R., Parikshak, N.N., Leppa, V., Ramaswami, G., Hartl, C., Schork, A.J., Appadurai, V., Buil, A., Werge, T.M., et al. (2018). Shared molecular neuropathology across major psychiatric disorders parallels polygenic overlap. Science *359*, 693–697. https://doi.org/10.1126/science.aad6469.

57. Xia, M., Liu, J., Mechelli, A., Sun, X., Ma, Q., Wang, X., Wei, D., Chen, Y., Liu, B., Huang, C.C., et al. (2022). Connectome gradient dysfunction in major depression and its association with gene expression profiles and treatment outcomes. Mol. Psychiatry *27*, 1384–1393. https://doi.org/10.1038/s41380-022-01519-5.

58. Swoboda, K.J., and Hyland, K. (2002). Diagnosis and treatment of neurotransmitter-related disorders. Neurol. Clin. *20*, 1143–1161. https://doi.org/10.1016/s0733-8619(02)00018-x.

59. Brown, R.P., and Mann, J.J. (1985). A clinical perspective on the role of neurotransmitters in mental disorders. Hosp. Community Psychiatry *36*, 141–150. https://doi.org/10.1176/ps.36.2.141.

60. Kato, T.A., Yamauchi, Y., Horikawa, H., Monji, A., Mizoguchi, Y., Seki, Y., Hayakawa, K., Utsumi, H., and Kanba, S. (2013). Neurotransmitters, psychotropic drugs and microglia: Clinical implications for psychiatry. Curr. Med. Chem. *20*, 331–344. https://doi.org/10.2174/0929867311320030003.

61. Liu, X., d'Oleire Uquillas, F., Viaene, A.N., Zhen, Z., and Gomez, J. (2022). A multifaceted gradient in human cerebellum of structural and functional development. Nat. Neurosci. *25*, 1129–1133. https://doi.org/10.1038/s41593-022-01136-z.

62. Larsen, B., Sydnor, V.J., Keller, A.S., Yeo, B.T.T., and Satterthwaite, T.D. (2023). A critical period plasticity framework for the sensorimotor-association axis of cortical neurodevelopment. Trends Neurosci. *46*, 847–862. https://doi.org/10.1016/j.tins.2023.07.007.

63. Kryazhimskiy, S., and Plotkin, J.B. (2008). The population genetics of dn/ds. PLoS Genet. *4*, e1000304. https://doi.org/10.1371/journal.pgen.1000304.

64. Wei, Y., de Lange, S.C., Scholtens, L.H., Watanabe, K., Ardesch, D.J., Jansen, P.R., Savage, J.E., Li, L., Preuss, T.M., Rilling, J.K., et al. (2019). Genetic mapping and evolutionary analysis of human-expanded cognitive networks. Nat. Commun. *10*, 4839. https://doi.org/10.1038/s41467-019-12764-8.

65. Won, H., Huang, J., Opland, C.K., Hartl, C.L., and Geschwind, D.H. (2019). Human evolved regulatory elements modulate genes involved in cortical expansion and neurodevelopmental disease susceptibility. Nat. Commun. *10*, 2396. https://doi.org/10.1038/s41467-019-10248-3.

66. Balsters, J.H., Cussans, E., Diedrichsen, J., Phillips, K.A., Preuss, T.M., Rilling, J.K., and Ramnani, N. (2010). Evolution of the cerebellar cortex: The selective expansion of prefrontal-projecting cerebellar lobules. Neuroimage *49*, 2045–2052. https://doi.org/10.1016/j.neuroimage.2009.10.045.

67. Margulies, D.S., Ghosh, S.S., Goulas, A., Falkiewicz, M., Huntenburg, J.M., Langs, G., Bezgin, G., Eickhoff, S.B., Castellanos, F.X., Petrides, M., et al. (2016). Situating the default-mode network along a principal gradient of macroscale cortical organization. Proc. Natl. Acad. Sci. USA *113*, 12574–12579. https://doi.org/10.1073/pnas.1608282113.

68. Nenning, K.H., Xu, T., Franco, A.R., Swallow, K.M., Tambini, A., Margulies, D.S., Smallwood, J., Colcombe, S.J., and Milham, M.P. (2023). Omnipresence of the sensorimotor-association axis topography in the human connectome. Neuroimage *272*, 120059. https://doi.org/10.1016/j.neuroimage.2023.120059.

69. Rieubland, S., Roth, A., and Häusser, M. (2014). Structured connectivity in cerebellar inhibitory networks. Neuron *81*, 913–929. https://doi.org/10.1016/j.neuron.2013.12.029.

70. Cerminara, N.L., Lang, E.J., Sillitoe, R.V., and Apps, R. (2015). Redefining the cerebellar cortex as an assembly of non-uniform purkinje cell microcircuits. Nat. Rev. Neurosci. *16*, 79–93. https://doi.org/10.1038/nrn3886.

71. Goulas, A., Changeux, J.P., Wagstyl, K., Amunts, K., Palomero-Gallagher, N., and Hilgetag, C.C. (2021). The natural axis of transmitter receptor distribution in the human cerebral cortex. Proc. Natl. Acad. Sci. USA *118*, e2020574118. https://doi.org/10.1073/pnas.2020574118.

72. Buckner, R.L., Krienen, F.M., Castellanos, A., Diaz, J.C., and Yeo, B.T.T. (2011). The organization of the human cerebellum estimated by intrinsic functional connectivity. J. Neurophysiol. *106*, 2322–2345. https://doi.org/10.1152/jn.00339.2011.

73. Zucchi, E., Ticozzi, N., and Mandrioli, J. (2019). Psychiatric symptoms in amyotrophic lateral sclerosis: Beyond a motor neuron disorder. Front. Neurosci. *13*, 175. https://doi.org/10.3389/fnins.2019.00175.

74. Kabiljo, R., Iacoangeli, A., Al-Chalabi, A., and Rosenzweig, I. (2022). Amyotrophic lateral sclerosis and cerebellum. Sci. Rep. *12*, 12586. https://doi.org/10.1038/s41598-022-16772-5.

75. Schmahmann, J.D. (2021). Emotional disorders and the cerebellum: Neurobiological substrates, neuropsychiatry, and therapeutic implications. Handb. Clin. Neurol. *183*, 109–154. https://doi.org/10.1016/B978-0-12-822290-4.00016-5.

76. Flores-Barrera, E., Thomases, D.R., Heng, L.J., Cass, D.K., Caballero, A., and Tseng, K.Y. (2014). Late adolescent expression of glun2b transmission in the prefrontal cortex is input-specific and requires postsynaptic protein kinase a and d1 dopamine receptor signaling. Biol. Psychiatry *75*, 508–516. https://doi.org/10.1016/j.biopsych.2013.07.033.

77. Alexander, M.P., Gillingham, S., Schweizer, T., and Stuss, D.T. (2012). Cognitive impairments due to focal cerebellar injuries in adults. Cortex *48*, 980–990. https://doi.org/10.1016/j.cortex.2011.03.012.

78. Villarroel, M.A., and Terlizzi, E.P. (2020). Symptoms of depression among adults: United States, 2019. NCHS Data Brief, 1–8.

79. Beyreli, I., Karakahya, O., and Cicek, A.E. (2022). Deepnd: Deep multi-task learning of gene risk for comorbid neurodevelopmental disorders. Patterns (N Y) *3*, 100524. https://doi.org/10.1016/j.patter.2022.100524.

80. Sydnor, V.J., Larsen, B., Seidlitz, J., Adebimpe, A., Alexander-Bloch, A.F., Bassett, D.S., Bertolero, M.A., Cieslak, M., Covitz, S., Fan, Y., et al. (2023). Intrinsic activity development unfolds along a sensorimotor-association cortical axis in youth. Nat. Neurosci. *26*, 638–649. https://doi.org/10.1038/s41593-023-01282-y.

81. Baum, G.L., Flournoy, J.C., Glasser, M.F., Harms, M.P., Mair, P., Sanders, A.F.P., Barch, D.M., Buckner, R.L., Bookheimer, S., Dapretto, M., et al. (2022). Graded variation in t1w/t2w ratio during adolescence: Measurement, caveats, and implications for development of cortical myelin. J. Neurosci. *42*, 5681–5694. https://doi.org/10.1523/JNEUROSCI.2380-21.2022.

82. Amare, A.T., Vaez, A., Hsu, Y.H., Direk, N., Kamali, Z., Howard, D.M., McIntosh, A.M., Tiemeier, H., Bültmann, U., Snieder, H., and Hartman, C.A. (2020). Bivariate genome-wide association analyses of the broad depression phenotype combined with major depressive disorder, bipolar disorder or schizophrenia reveal eight novel genetic loci for depression. Mol. Psychiatry *25*, 1420–1429. https://doi.org/10.1038/s41380-018-0336-6.

83. Bienias, K., Fiedorowicz, A., Sadowska, A., Prokopiuk, S., and Car, H. (2016). Regulation of sphingomyelin metabolism. Pharmacol. Rep. *68*, 570–581. https://doi.org/10.1016/j.pharep.2015.12.008.

84. Gualtieri, C.T. (2020). Genomic variation, evolvability, and the paradox of mental illness. Front. Psychiatry *11*, 593233. https://doi.org/10.3389/fpsyt.2020.593233.

85. Miller, D.J., Duka, T., Stimpson, C.D., Schapiro, S.J., Baze, W.B., McArthur, M.J., Fobbs, A.J., Sousa, A.M.M., Sestan, N., Wildman, D.E., et al. (2012). Prolonged myelination in human neocortical evolution. Proc. Natl. Acad. Sci. USA *109*, 16480–16485. https://doi.org/10.1073/pnas.1117943109.

86. Markello, R.D., Arnatkeviciute, A., Poline, J.B., Fulcher, B.D., Fornito, A., and Misic, B. (2021). Standardizing workflows in imaging transcriptomics with the abagen toolbox. Elife *10*, e72129. https://doi.org/10.7554/eLife.72129.

87. Burt, J.B., Helmer, M., Shinn, M., Anticevic, A., and Murray, J.D. (2020). Generative modeling of brain maps with spatial autocorrelation. Neuroimage *220*, 117038. https://doi.org/10.1016/j.neuroimage.2020.117038.

88. Diedrichsen, J., Balsters, J.H., Flavell, J., Cussans, E., and Ramnani, N. (2009). A probabilistic mr atlas of the human cerebellum. Neuroimage *46*, 39–46. https://doi.org/10.1016/j.neuroimage.2009.01.045.

89. Gu, Z. (2022). Complex heatmap visualization. iMeta *1*, e43. https://doi.org/10.1002/imt2.43.

90. Wu, T., Hu, E., Xu, S., Chen, M., Guo, P., Dai, Z., Feng, T., Zhou, L., Tang, W., Zhan, L., et al. (2021). Clusterprofiler 4.0: A universal enrichment tool for interpreting omics data. Innovation *2*, 100141. https://doi.org/10.1016/j.xinn.2021.100141.

91. Smith, S.M., Beckmann, C.F., Andersson, J., Auerbach, E.J., Bijsterbosch, J., Douaud, G., Duff, E., Feinberg, D.A., Griffanti, L., Harms, M.P., et al. (2013). Resting-state fmri in the human connectome project. Neuroimage *80*, 144–168. https://doi.org/10.1016/j.neuroimage.2013.05.039.

92. Glasser, M.F., Sotiropoulos, S.N., Wilson, J.A., Coalson, T.S., Fischl, B., Andersson, J.L., Xu, J., Jbabdi, S., Webster, M., Polimeni, J.R., et al. (2013). The minimal preprocessing pipelines for the human connectome project. Neuroimage *80*, 105–124. https://doi.org/10.1016/j.neuroimage.2013.04.127.

93. Van Essen, D.C., Ugurbil, K., Auerbach, E., Barch, D., Behrens, T.E.J., Bucholz, R., Chang, A., Chen, L., Corbetta, M., Curtiss, S.W., et al. (2012). The human connectome project: A data acquisition perspective. Neuroimage *62*, 2222–2231. https://doi.org/10.1016/j.neuroimage.2012.02.018.

94. Vos de Wael, R., Benkarim, O., Paquola, C., Lariviere, S., Royer, J., Tavakol, S., Xu, T., Hong, S.J., Langs, G., Valk, S., et al. (2020). Brainspace: A toolbox for the analysis of macroscale gradients in neuroimaging and connectomics datasets. Commun. Biol. *3*, 103. https://doi.org/10.1038/s42003-020-0794-7.

95. Coifman, R.R., Lafon, S., Lee, A.B., Maggioni, M., Nadler, B., Warner, F., and Zucker, S.W. (2005). Geometric diffusions as a tool for harmonic analysis and structure definition of data: Diffusion maps. Proc. Natl. Acad. Sci. USA *102*, 7426–7431. https://doi.org/10.1073/pnas.0500334102.

96. Yeo, B.T.T., Krienen, F.M., Sepulcre, J., Sabuncu, M.R., Lashkari, D., Hollinshead, M., Roffman, J.L., Smoller, J.W., Zöllei, L., Polimeni, J.R., et al. (2011). The organization of the human cerebral cortex estimated by intrinsic functional connectivity. J. Neurophysiol. *106*, 1125–1165. https://doi.org/10.1152/jn.00338.2011.

97. Diedrichsen, J. (2006). A spatially unbiased atlas template of the human cerebellum. Neuroimage *33*, 127–138.

98. Ritchie, M.E., Phipson, B., Wu, D., Hu, Y., Law, C.W., Shi, W., and Smyth, G.K. (2015). Limma powers differential expression analyses for rna-sequencing and microarray studies. Nucleic Acids Res. *43*, e47. https://doi.org/10.1093/nar/gkv007.

99. Liu, S., Abdellaoui, A., Verweij, K.J.H., and van Wingen, G.A. (2023). Gene expression has distinct associations with brain structure and function in major depressive disorder. Adv. Sci. *10*, e2205486. https://doi.org/10.1002/advs.202205486.

100. Miller, J.A., Ding, S.L., Sunkin, S.M., Smith, K.A., Ng, L., Szafer, A., Ebbert, A., Riley, Z.L., Royall, J.J., Aiona, K., et al. (2014). Transcriptional landscape of the prenatal human brain. Nature *508*, 199–206. https://doi.org/10.1038/nature13185.

101. Kumar, L., and E Futschik, M. (2007). Mfuzz: A software package for soft clustering of microarray data. Bioinformation *2*, 5–7. https://doi.org/10.6026/97320630002005.

102. Durinck, S., Moreau, Y., Kasprzyk, A., Davis, S., De Moor, B., Brazma, A., and Huber, W. (2005). Biomart and bioconductor: A powerful link between biological databases and microarray data analysis. Bioinformatics *21*, 3439–3440. https://doi.org/10.1093/bioinformatics/bti525.

103. Vogel, J.W., La Joie, R., Grothe, M.J., Diaz-Papkovich, A., Doyle, A., Vachon-Presseau, E., Lepage, C., Vos de Wael, R., Thomas, R.A., Iturria-Medina, Y., et al. (2020). A molecular gradient along the longitudinal axis of the human hippocampus informs large-scale behavioral systems. Nat. Commun. *11*, 960. https://doi.org/10.1038/s41467-020-14518-3.

STAR★METHODS

KEY RESOURCES TABLE

REAGENT or RESOURCE	SOURCE	IDENTIFIER
Deposited data		
Gene expression data from human brain tissues	Allen Human Brain Atlas (AHBA)	http://human.brain-map.org/; RRID:SCR_007416
Gene expression data from developmental human brain	BrainSpan	https://www.brainspan.org/; RRID:SCR_008083
Neuroimaging data from HCP	Human Connectome Project (HCP)	https://www.humanconnectome.org/; RRID:SCR_006942
Cerebellar cell type data	DropViz	http://dropviz.org/
Ex vivo psychiatric gene dysfunction	Middleton and Strick[18]	https://github.com/mgandal/Shared-molecular-neuropathology-across-major-psychiatric-disorders-parallels-polygenic-overlap
Code used	This paper	https://zenodo.org/records/10523603
Software and algorithms		
Python 3.10.8	Python	https://www.python.org/; RRID:SCR_008394
R 4.2	R Foundation	https://www.r-project.org/; RRID:SCR_001905
MATLAB	MathWorks	https://uk.mathworks.com/; RRID:SCR_001622
Abagen toolbox	Markello et al.[86]	https://github.com/netneurolab/abagen (https://doi.org/10.5281/zenodo.5129257); RRID:SCR_023832
Brain Surrogate Maps with Autocorrelated Spatial Heterogeneity (BrainSMASH) toolbox	Burt et al.[87]	https://github.com/murraylab/brainsmash
Gene set variation analysis (GSVA) package	Hänzelmann et al.[31]	https://bioconductor.org/packages/release/bioc/html/GSVA.html; RRID:SCR_021058
SUIT toolbox	Diedrichsen et al.[88]	https://www.diedrichsenlab.org/imaging/suit.htm; RRID:SCR_004969
ComplexHeatmap package	Gu[89]	https://bioconductor.org/packages/release/bioc/html/ComplexHeatmap.html; RRID:SCR_017270
ClusterProfiler package	Wu et al.[90]	https://guangchuangyu.github.io/software/clusterProfiler/; RRID:SCR_016884

RESOURCE AVAILABILITY

Lead contact

Further information and requests for resources should be directed to and will be fulfilled by the lead contact, Lingzhong Fan (lingzhong.fan@ia.ac.cn).

Materials availability

This study did not generate unique reagents.

Data and code availability

- All data used in this study were publicly available and presented in the article and the Supplementary materials. These accessions for the datasets are listed in the Key resources table.
- All original code has been deposited at https://github.com/FANLabCASIA/Gene2predictCerebellarSA, as well as at Zendo as https://doi.org/10.5281/zenodo.10523603, and is publicly available as of the date of publication.
- Any additional information required to reanalyze the data reported in this paper is available from the lead contact upon request.

METHOD DETAILS

Experimental design

The schematic of the experimental design that addressed three progressive questions is depicted in Figure 1. Question 1 (Figure 1A): Could the sensorimotor-association axis (SA axis) of the adult human cerebellum extracted from the functional gradient (FG) be significantly predicted by gene expression? We leveraged the partial least-squares regression (PLSR) to predict the FG using sample-wise transcriptome gene expression. Question 2 (Figure 1B): What intermediate biological principles mediate this SA axis, and is there a link between evolution and neuropsychiatric diseases of the cerebellum and these spatio-molecular profiles? Gene set variation analysis (GSVA), an *ex vivo* psychiatric gene dysregulation dataset, a developmental transcriptome dataset, and the evolution rate of genes were introduced to the significant gene expression along the SA axis to explore this question. Question 3 (Figure 1C): What is the involvement of the cerebral cortex in the cerebellar SA axis at the genetic and functional connectivity (FC) levels? The correlation between the regression coefficient of significant genes and the gene expression of cerebral cortical samples, as well as of the FC between significantly engaged cerebral cortical samples and the cerebellum, were examined.

The FG of the human cerebellum

The minimally preprocessed[91,92] Human Connectome Project (HCP) S1200 release dataset,[93] which has 1,018 subjects (aged from 22 to 37 years old) with both structural MRI and resting-state functional MRI (rs-fMRI) data, was leveraged to get a 2 mm voxel-wise, group-averaged, preprocessed dense connectome that includes correlation values for each cerebellar voxel with the extra-cerebellar voxels. It provides a spatial distribution of FCs for each cerebellar voxel with extra-cerebellar voxels (a connectivity profile). Then, an affinity matrix was created using the cosine distance to determine the consistency between pairs of voxels, indicating the similarity of their connection patterns. To ensure that only the strong, potentially less noisy connections contribute to the later manifold solution,[94] the affinity matrix was thresholded at the 90th percentile to transform it into a sparse affinity matrix.[7] Last, a nonlinear dimensionality reduction technique, i.e., diffusion map embedding,[95] was leveraged to recover a low-dimensional embedding from the high-dimensional sparse affinity matrix. The diffusion map embedding results in the first component (or first gradient, primary gradient), which reflects as much of the variance of the data as possible.[67] Under this constraint, all the subsequent components are orthogonal and designed to account for the highest possible variability. Noteworthy is that the first gradient explains the greatest amount of variance in the cerebello-exracerebellar functional connectivity (Figure S1B). We focused on the first gradient, and thus the FG of the current analysis is referred to as the first gradient. The results were visualized as cerebellar flat maps using the SUIT toolbox.[88]

For a quantitative demonstration of the primary assumption that FG reflects an SA axis, we conducted two analyses to explore the relationship between cerebellar FG with task activation (Figure S1C) and cerebral cortical connectivity (Figure 2A, right). For the task activation, we tried to give a quantitative demonstration using another modality, i.e., task-based fMRI. We assigned the cerebellar voxels to the independent task-based MDTB functional parcellation[32] and calculated the mean, median, and range of the FG values for the voxels within each MDTB ROI activated during different tasks. For the cerebral cortical connectivity, we generated 100 ROIs along the cerebellar FG. Firstly, we sorted the voxels by the FG value and divided them into 100 ROIs. Then, we calculated the functional connectivity (FC) between these 100 cerebellum ROIs and the cerebral cortex. The rs-fMRI of 100 unrelated subjects (U100) was obtained from the minimally preprocessed[91,92] HCP S1200 release dataset.[93] Then, we could evaluate the Fisher z transformed correlation between these 100 ROIs with the cerebral cortex across 100 subjects. These correlations for all 100 subjects were combined to calculate the t score value for every cerebral cortex voxel. The binarized maps of significantly functionally connected cerebral cortex regions were generated using voxel-wise family-wise error corrected by Bonferroni $p < .001$. The significant FC between these 100 cerebellar FG-sorted ROIs with cerebral cortex was quantified at the 7-network level of a cerebral cortical functional networks atlas,[96] and the networks were sorted by the cerebral cortical SA axis.[67]

Human transcriptome data

The Allen Human Brain Atlas (AHBA)[28] dataset, available to the public at http://www.brain-map.org, offers normalized microarray gene expression information from six adult donors (ages 24, 31, 34, 49, 55, and 57 years; n = 4, left hemisphere only; n = 2, both left and right hemispheres). Demographic details are listed in Table S1. The Institutional Review Boards of the Maryland Department of Health and Hygiene, the University of Maryland Baltimore, and the University of California Irvine approved the collection of tissue samples. Informed consent was obtained from the next-of-kin of the deceased individuals.[28] Although AHBA provides gene expression from only six adult donors, it still has many unprecedented advantages. While some existing human gene expression atlases cover multiple brain regions, only the AHBA delivers high-resolution coverage of nearly the entire brain.[25] It includes the expression of more than 20,000 genes taken from 3,702 spatially distinct tissue samples[28] ranging from the cerebral cortex to the cerebellum.

As utilized in Markello et al.,[86] the pre-processing pipeline included probe-to-gene re-annotations and sample selection using an intensity-based filtering of probes at a threshold of 0.5. It also included the removal of samples that had an inconsistent hemisphere annotation or MNI coordinates (hemisphere = = "L" & mni_x > 0 | hemisphere = = "R" & mni_x < 0). Probe selection included using differential stability for the data from all donors. Gene normalization was done using a scaled robust sigmoid transform.[25] The rest of the parameters were left at their default settings. This preprocessing was achieved by using the get_samples_in_mask function of the

abagen toolbox[86] with no mask input. The output of the pre-processing pipeline included a gene-by-sample expression matrix with 15,624 genes and 3604 samples across all donors combined with the sample annotation matrix.

We obtained the 337 samples belonging to the cerebellar cortex based on the slab_type equal to "CB" (cerebellum) function and removed the cerebellar nucleus by filtering out the samples whose structure name contained the keyword "nucleus," based on the sample annotation matrix given by abagen. Although the corrected sample coordinates after manually updating the non-linear diffeomorphic registration of all the donors were used as suggested by abagen,[86] many issues specific to the alignment of the cerebellum were still not taken into account, not to mention that the scan of donor 15697 showed a deformed cerebellum. Therefore, we re-ran the preprocessing of the six donor T1 images using the SUIT toolbox to obtain more accurate coordinates, which were optimized for the cerebellum of the 337 cerebellar samples. This method preserved the anatomical details of the cerebellar structures by a nonlinear alignment algorithm to ameliorate possible phenomena resulting from improved lacunar superposition, spatial variation, and overlap of the deep cerebellar nuclei. The main steps of this preprocessing included alignment, segmentation, and deformation.[97]

Then we assigned an FG value to each of the 337 cerebellar samples by averaging the FG values of voxels less than 4 mm away from the corrected sample SUIT coordinates. It is worth pointing out that the scale of the FG is arbitrary, we normalized the FG to the range from 0 to 1 to reduce the unwanted effect of adding positive and negative values when we averaged the FG of voxels less than 4 mm away (the original values of the FG are shown in Figure S1). For the samples with FG values equal to 0, we also manually removed those that were not on the cerebellum based on their visible location, resulting in 317 cerebellar samples.

Prediction of FG using the transcriptome

Based on the pre-processed 15624 genes × 317 cerebellar samples gene expression matrix, we leveraged the partial least-squares regression (PLSR) model to predict the human cerebellar SA axis, which is well established by FG. The optimal component number from the PLSR was validated by a 100 times nested 10-fold cross-validation (CV). In brief, in the initial 10-fold CV, the samples were randomly split into 9-fold for training and 1-fold for testing. Then the 9-fold training samples underwent a nested 10-fold CV for which the mean square error (mse) was obtained for a component number ranging from 1 to 10 to derive the optimal component number within the initial 9-fold training samples. Next, the optimal component number within the initial 9-fold training samples was used to test the correlation between the observed FG and the predicted FG of the initial 1-fold training samples. We repeated this nested 10-fold CV 100 times to obtain the optimal component number (Figure S2).

To test model generalizability, we repeated a 10-fold CV strategy 101 times (since data division could influence performance and an odd number of repeats was chosen to enable straightforward identification of the the median model). The correlation coefficients (r) between the predicted and actual FG were calculated, and the median of the r values across the 101 repetitions was referred to as the prediction performance. To test the significance of the prediction performance while considering the spatial autocorrelation, we leveraged Brain Surrogate Maps with Autocorrelated Spatial Heterogeneity (BrainSMASH)[87] to generate 10,000 surrogate FG maps, which retained the spatial autocorrelation of the voxel-level FG map. These 10,000 surrogate FG maps were used to assign the surrogate FG value to the 317 cerebellar samples. Then we re-ran the PLSR model with the same split strategy, thus generating an empirical null distribution of the prediction performance while considering the spatial autocorrelation. The p value that controlled the spatial auto-correlation (p_{sa}) was defined as the proportion of correlation values produced by the surrogate maps that exceeded the correlation coefficient for the actual data. Second, we performed a leave-one-donor-out CV to see whether a model trained on the samples of five donors could predict the sample-wise FG of the sixth donor (Figure S3). Note that the number of samples varied considerably across donors. The final model used for all the subsequent analyses utilized all the samples.

The regression coefficient of each gene in the PLSR model represented the degree of contribution of each gene to the prediction of the FG. Thus, the regression coefficient could act as the gene contribution indicator (GCI). To test the significance of the GCI and identify the significant genes, a permutation of BrainSMASH, which preserves the spatial auto-correlation of the FG, was also used to construct the null distribution of GCI for each gene, and the p_{sa} for each gene was defined as the proportion of the absolute value of GCI from the null distribution that exceeded the absolute value of the true GCI. Then the p_{sa} of GCI was adjusted by Bonferroni correction (smaller than .05 divided by 15624 was considered significant), and the set of the genes with a significant GCI was referred to as GCI_{sig} for simplicity and fluency.

Gene set variation analysis (GSVA)

The GSVA[31] provides more power for assaying subtle alterations in biological activity over a sample population than gained by using only the correlated genes. It thus was introduced as an attempt to cope with the conventional limits of imaging-transcriptome studies. We mainly included three steps in the current study. First, bioinformatics datasets, including gene ontology (GO),[33,34] Kyoto Encyclopedia of Genes and Genomes (KEGG),[35] and cerebellar cell types data from DropViz,[36] were utilized to group genes into gene sets based on their biological functions. Then the genes × samples expression matrix was transformed into a genesets × samples enrichment score matrix based on the kernel estimation of the cumulative density function to show the variation in the gene set along with the samples. Last, differential analysis[98] was leveraged to obtain significantly expressed functional gene sets between different sample types.

Specifically, the 317 samples were reordered based on their FG value and then divided into 20 bins, with the gene expression and FG averaged for each bin. The reasons for the bin-based analysis include that the GSVA algorithm's strategy of requiring a sample

size greater than 10 and larger than 60 does not increase the statistical power but increases empirical type-I errors. And earlier research confirmed that a bin-based correlation analysis could improve statistical power and lower noise.[51,67,99] Alternative numbers of bins (30, 40, 50, and 60, Figures S4, S5, S6, and S7) were also applied to test the stability across choices of bin numbers. Taking 20-bin as an example, GSVA transformed the GCI_{sig} × 20 bins gene expression matrix into a genesets × 20 bins enrichment score matrix. Then, a differential analysis was utilized to obtain the significantly expressed gene sets between the sensorimotor and association samples. A fold change >1 and $p < .05$ (FDR corrected) was used as an indicator to threshold the significant gene set. Whether the sample belongs to the association or sensorimotor region was determined based on whether the FG after averaging was greater than 0.5 or not. This binary category was only used as an approximate indicator of the characteristics of the two ends of the SA axis.[4] The significant gene set expression along the SA axis was visualized by ComplexHeatmap[89] for the sample hierarchical clustering method with default settings. To facilitate visualization, for some categories with a greater number of results, such as GO, we only showed the top 20 in the heatmap (full results can be found in Datas S2, S3, S4, S5, S6, S7, S8, and S9).

Relationships with neuropsychiatric disorders

To determine the role of GCI_{sig} in disease, we utilized two different strategies. In the first strategy, we adopted the statistical abilities of GSVA, i.e., to mine out subtle changes in the samples, to see the changes in disease along the cerebellar SA axis by replacing the dataset with a disease gene network (DisGeNET).[49] The DisGeNET dataset is one of the richest and most publicly accessible biomedical resources. It includes a broad range of disease phenotypes associated with human genomics: actual diseases, disease symptoms, and abnormal phenotypes that are observed as disease manifestations, as well as normal traits and phenotypes that are currently explored in large-scale Genome-Wide Association Studies.[49] The validation of the different bins was the same as before (Figure S7).

Another strategy, i.e., *ex vivo* psychiatric gene dysfunction, was used as a focus to investigate the relationship between GCI and psychiatric disorders. The *ex vivo* psychiatric gene dysfunction was obtained from Gandal et al.[56] (https://github.com/mgandal/Shared-molecular-neuropathology-across-major-psychiatric-disorders-parallels-polygenic-overlap) and provided differential gene expression information across five major psychiatric disorders, i.e., major depression (MDD), bipolar disorder (BD), autistic spectrum disorder (ASD), schizophrenia (SCZ), and alcohol abuse disorder (AAD), compared with matched controls. The $\log_2$ fold change ($\log_2$ FC) was obtained from a linear mixed-effects model and represents the extent to which a gene is up or down-regulated in each psychiatric population.[56] As found by Anderson et al.[51] and Liu et al.,[99] the $\log_2$ FC values of most genes were distributed around zero. Thus, a gene-wise transcriptional correlation analysis with $\log_2$ FC could cause bias in estimating the correlation due to noise, so a bin-based correlation analysis was further applied. Specifically, the overlapped genes were reordered based on their GCI value and then divided into 40 bins, with GCI and $\log_2$ FC averaged for each bin. Then the correlation between the GCI underlying the *in vivo* SA axis and the *ex vivo* $\log_2$ FC for each psychiatric disorder was examined. Alternative number of bins (20, 60, 80, and 100) were also applied to test the stability across choices of bin numbers (Figure S8).

Developmental clustering and evolution rate

To investigate the overall developmental features of GCI_{sig}, we utilized the BrainSpan[100] dataset, which provides gene expression along the lifespan (42 donors, ages 8 post-conception weeks to 40 years). Because it contains 524 samples covering the whole brain, we only focused on the 34 cerebellar samples, and multiple samples for the same age were averaged. After removing the duplicates, 891 genes were found to overlap between BrainSpan and AHBA GCI_{sig}, and an 891 genes × 28 ages matrix was used for a clustering analysis to explore the overall trajectory. The fuzzy clustering algorithm Mfuzz[101] was leveraged because it is good at clustering based on temporal expression information: since it is common for different classes to overlap in temporal expression data, it is better to use soft clustering rather than hard clustering.[101] The optimal cluster number, i.e., 2, was chosen based on the total within-clusters sum of squares and the average silhouette method (Figure S9A). Meanwhile, the 8 cluster results are also shown in Figure S9B because the total within-clusters sum suggests that 8 is another good solution. After the initial clustering, we applied the over-representation analysis (ORA) gene enrichment by ClusterProfiler[90] to obtain the potential biological explanation, such as GO and KEGG, for each cluster.

The evolutionary rate of genes[63] is a widely used measure to quantify the speed of evolutionary change. It is defined as the ratio between the rate of its nonsynonymous and its synonymous rates, i.e., dN/dS. A $dN/dS < 1$ indicates a negative purifying selection and thus is more conserved, = 1 indicates neutral evolution and no change between two species, whereas >1 indicates positive selection and thus is less conserved.[63] Two species, i.e., mouse and chimpanzee, were selected to test the difference in the evolution rate of GCI_{sig} between mouse-human and chimpanzee-human using the human genome as a reference. Based on BioMart,[102] we first obtained the homologous genes between mice and humans and then calculated the dN/dS values for GCI_{sig}, i.e., their mouse-human evolutionary rates. We then repeated this procedure for the chimpanzee-human data. Welch's t test was used to compare the dN/dS ratio between the mouse-human and chimpanzee-human rates.

Cerebral cortical interaction with GCI_{sig}

To explore how the relationship between GCI_{sig} and the cerebellar SA axis is represented in the cerebral cortex, we first obtained the cerebral cortical sample-wise gene expression from AHBA. The pre-processing pipeline was consistent with that used for the cerebellum. By this procedure, we derived the pre-processed 15,624 genes × 1539 samples of the cerebral cortical matrix.

Then we calculated the correlation between each cerebral cortical gene expression, i.e., 1024 genes × 1 sample, with the GCI value of 1024 genes from GCI_{sig} to obtain the correlation with GCI_{sig} for 1539 cerebral cortical samples. And this correlation was referred to as the Cerebellar Hierarchical Representative Index of Similarity (CHRIS), a value representing the degree to which the genomic signature of the cerebellar SA axis is represented in the gene expression profile of a cerebral cortical sample.[103] The CHRIS could also indicate the similarity between a given cerebral cortical sample's gene expression and the gene expression along the cerebellar SA axis. Thus, a negative CHRIS ($CHRIS^-$) means a higher genetic similarity with the sensorimotor cerebellum, and a positive CHRIS ($CHRIS^+$) means a higher genetic similarity with the association cerebellum. The significance of CHRIS was evaluated by Bonferroni correction, whose correlation significance $p < (.05/1539)$ was referred to as significant, and the set of the cerebral cortical samples with significant CHRIS was named $CHRIS_{sig}$. $CHRIS_{sig}^-$ and $CHRIS_{sig}^+$ indicated a more significant similarity with the sensorimotor and association areas of the cerebellum, respectively. Meanwhile, the distribution of $CHRIS_{sig}$ was quantified at the 7-network level of the cortical functional networks atlas[96] to obtain a detailed visualization of $CHRIS_{sig}$ across the 7 networks. Assigning each sample coordinate to the 7-network parcellation enabled us to obtain the sum of the $CHRIS_{sig}$ for all the samples within the same network.

Next, we wanted to investigate whether there is any difference in FC between $CHRIS_{sig}^-$ and $CHRIS_{sig}^+$ as they each differentially genetically correlate with the sensorimotor and association areas of the cerebellum, respectively. The rs-fMRI of 100 unrelated subjects (U100) was obtained from the minimally preprocessed[91,92] HCP S1200 release dataset.[93] The seeds were defined by the combination of MNI coordinates of the samples identified as $CHRIS_{sig}^-$ and $CHRIS_{sig}^+$, respectively, so we had two seeds in total. To accomplish this, the AHBA was resampled to a 2 mm resolution to calculate the FC using HCP U100. Taking the $CHRIS_{sig}^+$ as an example, coordinates of 115 samples which belong to the $CHRIS_{sig}^+$ constitute the ROI for $CHRIS_{sig}^+$. Then we could evaluate the Fisher z transformed correlation between $CHRIS_{sig}^+$ ROI with the cerebellum across 100 subjects. These correlations for all 100 subjects were combined to calculate a t score value for every cerebellar voxel. The voxel-wise family-wise error corrected by Bonferroni $p < .001$ was utilized to generate the binarized maps of the significantly functionally connected cerebellar regions to $CHRIS_{sig}^-$ and $CHRIS_{sig}^+$. Finally, the distribution of the significant FC with $CHRIS_{sig}$ was quantified at the 7-network level of a cerebellar functional networks atlas.[72]

QUANTIFICATION AND STATISTICAL ANALYSIS

The generalizability of the PLSR model was evaluated using an embedded 10-fold CV, with the correlation between actual and predicted FG as the prediction performance. The significance of the prediction performance was determined by the BrainSMASH,[87] which controlled the spatial auto-correlation (p_{sa}). The significance of GCI and CHRIS was determined by $p_{sa} < .05$ after Bonferroni correction for multiple comparisons. The robustness of GSVA and *ex vivo* gene dysfunction analysis was evaluated by alternate numbers of bins. Welch's t test was used to compare the *dN/dS* ratio between the mouse-human and chimpanzee-human rates. For the FC calculation, the voxel-wise family-wise error corrected by Bonferroni $p < .001$ was utilized to generate the binarized maps of the significantly functionally connected voxels. Additional details for each analysis are provided in the relevant sections above.